

RESEARCH ARTICLE

Environment-induced same-sex mating in the yeast *Candida albicans* through the Hsf1–Hsp90 pathway

Guobo Guan^{1,2}, Li Tao³, Huizhen Yue^{1,2}, Weihong Liang^{1,2}, Jiao Gong^{1,2}, Jian Bing¹, Qiushi Zheng^{1,2}, Amanda O. Veri⁴, Shuru Fan^{1,2}, Nicole Robbins⁴, Leah E. Cowen⁴, Guanghua Huang^{3,1,2*}

1 State Key Laboratory of Mycology, Institute of Microbiology, Chinese Academy of Sciences, Beijing, China, **2** University of Chinese Academy of Sciences, Beijing, China, **3** State Key Laboratory of Genetic Engineering, School of Life Sciences, Fudan University, Shanghai, China, **4** Department of Molecular Genetics, University of Toronto, Toronto, Ontario, Canada

☉ These authors contributed equally to this work.

* huanggh@im.ac.cn



OPEN ACCESS

Citation: Guan G, Tao L, Yue H, Liang W, Gong J, Bing J, et al. (2019) Environment-induced same-sex mating in the yeast *Candida albicans* through the Hsf1–Hsp90 pathway. *PLoS Biol* 17(3): e2006966. <https://doi.org/10.1371/journal.pbio.2006966>

Academic Editor: Anita Sil, UCSF, United States of America

Received: June 13, 2018

Accepted: February 13, 2019

Published: March 13, 2019

Copyright: © 2019 Guan et al. This is an open access article distributed under the terms of the [Creative Commons Attribution License](https://creativecommons.org/licenses/by/4.0/), which permits unrestricted use, distribution, and reproduction in any medium, provided the original author and source are credited.

Data Availability Statement: The RNA-seq dataset has been deposited into the NCBI Gene Expression Omnibus (GEO) portal (accession# GSE119165).

Funding: National Natural Science Foundation of China <http://www.nsf.gov.cn/> (grant number 31625002, 31370175, 31600121, 31570139). Grant Number 31625002 and 31370175 to GH; Grant Number 31600121 to GG; Grant Number 31570139 to LT. The funder had no role in study design, data collection and analysis, decision to publish, or preparation of the manuscript. National

Abstract

While sexual reproduction is pervasive in eukaryotic cells, the strategies employed by fungal species to achieve and complete sexual cycles is highly diverse and complex. Many fungi, including *Saccharomyces cerevisiae* and *Schizosaccharomyces pombe*, are homothallic (able to mate with their own mitotic descendants) because of homothallic switching (HO) endonuclease-mediated mating-type switching. Under laboratory conditions, the human fungal pathogen *Candida albicans* can undergo both heterothallic and homothallic (opposite- and same-sex) mating. However, both mating modes require the presence of cells with two opposite mating types (*MTLa/a* and α/α) in close proximity. Given the predominant clonal feature of this yeast in the human host, both opposite- and same-sex mating would be rare in nature. In this study, we report that glucose starvation and oxidative stress, common environmental stresses encountered by the pathogen, induce the development of mating projections and efficiently permit same-sex mating in *C. albicans* with an “a” mating type (*MTLa/a*). This induction bypasses the requirement for the presence of cells with an opposite mating type and allows efficient sexual mating between cells derived from a single progenitor. Glucose starvation causes an increase in intracellular oxidative species, overwhelming the Heat Shock transcription Factor 1 (Hsf1)- and Heat shock protein (Hsp)90-mediated stress-response pathway. We further demonstrate that *Candida* TransActivating protein 4 (Cta4) and Cell Wall Transcription factor 1 (Cwt1), downstream effectors of the Hsf1–Hsp90 pathway, regulate same-sex mating in *C. albicans* through the transcriptional control of the master regulator of a-type mating, *MTLa2*, and the pheromone precursor-encoding gene Mating α factor precursor (*MF α*). Our results suggest that mating could occur much more frequently in nature than was originally appreciated and that same-sex mating could be an important mode of sexual reproduction in *C. albicans*.

Science and Technology Major Project <http://program.most.gov.cn/> (grant number 2018ZX10101004-003-002). Received by GH. The funder had no role in study design, data collection and analysis, decision to publish, or preparation of the manuscript.

Competing interests: The authors have declared that no competing interests exist.

Abbreviations: ACT1, ACTin 1; AIF1, Apoptosis-Inducing Factor 1; Arg, arginine; Bar1, BARRIER 1; CEK, Candida ERK-family protein kinase; ChIP, chromatin immunoprecipitation; Cta4, *Candida* TransActivating protein 4; Cwt1, Cell Wall Transcription factor 1; DIC, differential interference contrast; Dox, doxycycline; ERK, ERK-family protein kinase; FACS, Fluorescence-activated cell sorting; FDR, False Discovery Rate; FIG1, Factor-Induced Gene 1; FPKM, fragments per kb per million reads; FUS1, cell FUSion 1; GFP, green fluorescent protein; GPI, glycosylphosphatidylinositol; GST3, Glutathione S-transferase 3; His, histidine; HMX1, HeMe oXygenase; HO, Homothallic switching; Hsf1, Heat Shock transcription Factor 1; Hsp90, Heat shock protein; IP, immunoprecipitation; KAR2, KARyogamy; MAP, mitogen-activated protein; MAT α , Mating type α ; MFA1, Mating type A1; MFA, Mating α factor precursor; MTL, Mating type locus; Myc, Myc epitope tag; NA, not analyzed; NADH, Nicotinamide adenine dinucleotide; Ofr1, Opaque Formation Regulator 1; orf19.3475, *Candida* gene *orf19.3475*; p, mating projection; pACTS, plasmid pACTS; pACT1, plasmid pACT1; PAS, Per-Arnt-Sim; PI, propidium iodide; PST2, Protoplasts-Secreted 1; qRT-PCR, quantitative reverse transcription PCR; RNA-Seq, RNA sequencing; ROS, reactive oxidative species; SCD, synthetic complete medium; SDS, sodium dodecyl sulfate; SIS1, Sit4 Suppressor; SOD5, SuperOxide Dismutase 5; SSA2, Stress-Seventy subfamily A; STE2, STERile 2; TAP, Tandem affinity purification; TCA, tricarboxylic acid; tetON, tetracycline-induced; tetON-HSF1/hsf1, *tetON*-promoter-controlled conditional expression strain of *HSF1*; WOR1, White-Opaque Regulator 1; WT, wild type; Yci1, Dipeptidyl aminopeptidase Yci1; YPD-K, 1% yeast extract, 2% peptone, 2% glucose, 0.25% K₂HPO₄; YP-K, 1% yeast extract, 2% peptone, 0.25% K₂HPO₄.

Author summary

Candida albicans is notorious as a human fungal pathogen that causes millions of incidents of thrush and systemic infection every year. Sexual reproduction plays a pivotal role in the biology and survival of pathogenic fungal pathogens. However, *C. albicans* is predominantly clonal, suggesting that mating and recombination between isolates would be rare in nature. Here, we report that environmental stresses induce the development of mating projections and efficient same-sex mating in *C. albicans*. This induction represents a novel mode of homothallism that is independent of the HO endonuclease-mediated mating-type switching observed in *Saccharomyces cerevisiae* and *Schizosaccharomyces pombe*. This represents a seminal example of how an environmentally relevant stress induces homothallic mating in fungi.

Introduction

Sexual reproduction is a driving force for evolution and is prominent in eukaryotic organisms, with fungi adopting highly diverse strategies for sexual mating and reproduction [1, 2]. The human fungal pathogen *C. albicans* is a leading cause of death due to mycotic infection, with mortality rates approaching 40%, even with current treatments [3]. *C. albicans* has long been thought to be asexual until the discovery of a highly complex parasexual program. In *C. albicans*, heterothallic (opposite-sex) mating between diploid **a** and α cells occurs to generate tetraploid **a**/ α intermediates [4, 5]. These tetraploid mating products undergo a parasexual process of concerted chromosome loss to generate diploid and aneuploid progeny rather than adopting a more traditional meiotic cycle [6, 7]. As an additional layer of complexity, an epigenetic switch from the white cell type to the opaque cell type is required for efficient mating to occur [8]. Opaque **a** and α cells secrete a sex-specific pheromone and induce the formation of mating projections in cells with an opposite Mating type locus (*MTL*) type, thus initiating cell fusion and mating [9]. Besides differences in mating competency, white and opaque cells also differ in a number of aspects, including metabolic profiles, filamentation ability, susceptibility to antifungals, interactions with host immune cells, and virulence in different infection models [10–12].

Given the predominately clonal nature of *C. albicans* [13, 14], the frequency with which heterothallic mating occurs in nature appears remarkably low. In the model yeast *S. cerevisiae*, most natural isolates are homothallic and able to undergo clonal mating because of the expression of homothallic switching (HO) endonuclease and mating-type switching [1]. However, *C. albicans* does not have a homolog of HO endonuclease and is unable to undergo mating-type switching and subsequent clonal mating [15]. Although same-sex mating (homothallism) has been reported in *C. albicans*, this unisexual mating has only been observed between two **a** cells, when α cells are present and secrete α -pheromone (ménage à trois mating), or in strains in which the BARRIER 1 (Bar1) protease that degrades α -pheromone has been inactivated [16]. However, there is no evidence of natural ménage à trois mating, and no natural mutants of *BARI* have been reported. Given the barriers to opposite- and same-sex mating, the biological relevance of sexual reproduction in *C. albicans* remains elusive.

Although *C. albicans* mating seems to be rare in nature, environmental stressors have been reported to promote loss of heterozygosity at the *MTL*, drive white-to-opaque switching, and result in concerted chromosome loss, suggesting that stress may be a trigger for sexual reproduction [17]. Nutrient starvation and oxidative stresses are two of the most common environmental stressors experienced by *C. albicans* in nature. Here, we establish that glucose starvation and oxidative stress efficiently induce the expression of sexual pheromone

precursors, leading to the formation of mating projections and enabling homothallic mating in *C. albicans*. A core cellular stress-responsive pathway, mediated by the molecular chaperone Hsp90 and the heat-shock transcription factor Hsf1, is involved in this regulation through the downstream regulator Cwt1. Cwt1 functions through the direct control of the master regulator of a-type mating *MTLa2*, which regulates the expression of pheromone-encoding genes. Our study identifies a mechanism by which mating could occur much more frequently in nature than was originally appreciated, uncovers a core cellular stress-response pathway regulating this response, and sheds new light, to our knowledge, on the biology of *C. albicans*.

Results

Glucose starvation triggers the development of mating projections in *C. albicans*

Despite the fact that cellular stressors promote loss of heterozygosity at the *MTL* and induce the white-to-opaque switch [17, 18], there still remains no evidence to directly support the hypothesis that environmental perturbations regulate sexual mating in *C. albicans*. In the human host, *C. albicans* resides on mucosal surfaces, niches that are often glucose limited [19]. Therefore, we cultured *C. albicans* cells in the absence of glucose but in the presence of 0.25% K_2HPO_4 , which acts as a pH-buffering reagent. We named this modified medium as YP-K (1% yeast extract, 2% peptone, 0.25% K_2HPO_4 , w/v) and the control medium as YPD-K (1% yeast extract, 2% peptone, 2% glucose, 0.25% K_2HPO_4 , w/v). Opaque cells were used for all experiments in this study because they are the mating-competent form in *C. albicans* [8]. Upon spotting an *MTLa/a* *C. albicans* strain (GH1013) [20], we noted a wrinkled colony morphology on YP-K agar after five days of growth (Fig 1A). Surprisingly, a portion of cells

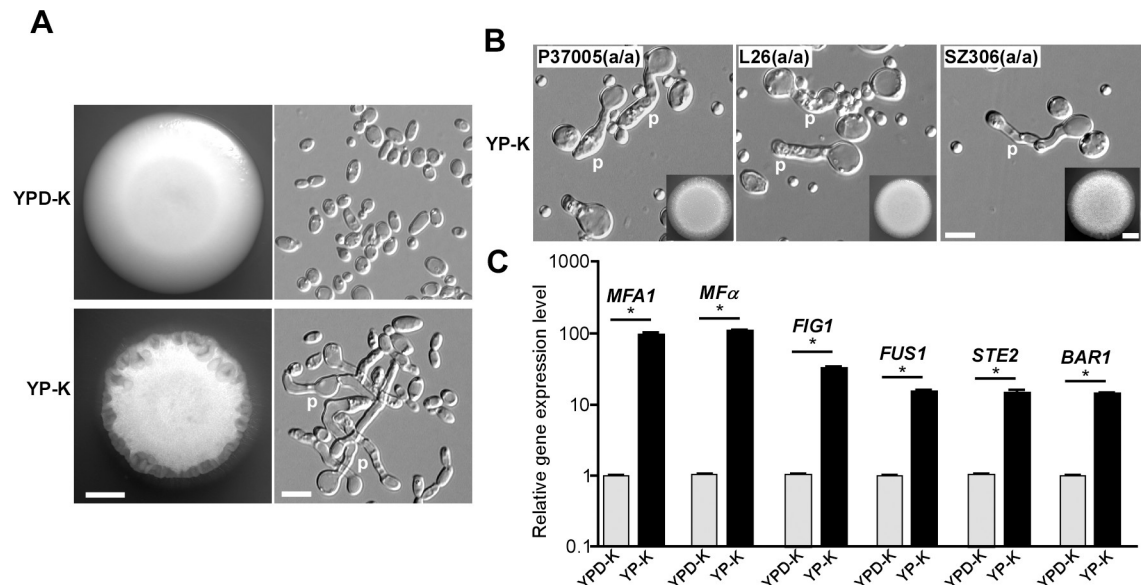


Fig 1. Glucose starvation promotes efficient polarized cell growth and induces the expression of mating-related genes in *MTLa/a* cells of *C. albicans*. (A) Morphologies of the laboratory strain GH1013 (*MTLa/a*) grown on YPD-K and YP-K media. 1×10^5 cells were spotted on YPD-K and YP-K media and cultured at 25°C for five days. Scale bar for colonies (left panels), 2 mm; scale bar for cells (right panels), 10 μ m. (B) Morphologies of three clinical *C. albicans* strains (*MTLa/a*) grown on YP-K medium at 30°C for four days. Scale bar for colonies (inset), 2 mm; scale bar for cells, 10 μ m. (C) Relative expression levels of mating-related genes normalized to *ACT1*. Cells of GH1013 were used, and culture conditions were same as described in panel (A). Error bars represent standard errors of technical duplicates. * $p < 0.05$, two-tailed Student *t* test. Experiment was repeated in a biological replicate, and a representative image is shown. The numerical data are presented in S3 Data. *ACT1*, ACTin 1; Bar1, BARrier 1; *FIG1*, Factor-Induced Gene 1; *FUS1*, cell FUSion 1; *MFA1*, Mating type A1; *MFα*, Mating α factor precursor; *MTL*, Mating type locus; p, mating projection; *STE2*, STErile 2; YPD-K, yeast extract-peptone-glucose- K_2HPO_4 ; YP-K, yeast extract-peptone- K_2HPO_4 .

<https://doi.org/10.1371/journal.pbio.2006966.g001>

underwent polarized cell growth (Fig 1A) that was elongated and irregular in shape, closely resembling mating projections as opposed to the typical hyphal morphology [21]. When the same strain was cultured on the glucose-containing YPD-K medium, the colonies remained smooth, and cells were exclusively in the yeast form (Fig 1A). This was a dose-dependent effect because incremental increases in glucose levels resulted in incremental decreases in the number of polarized cells observed (S1 Fig). We also observed the development of polarized cells on YP-K medium for three independent clinical isolates of *C. albicans* with an *MTLa/a* genotype (P37005, L26, and SZ306) (Fig 1B), suggesting that this inducing effect of glucose starvation is a general feature in *MTLa/a* strains. The induction of mating projections was not observed in any *MTLa/α* and *MTLα/α* strains under the same culture conditions.

To verify that the elongated cells were true mating projections but not pseudohyphae or true hyphae, we examined the relative expression of mating-related genes using quantitative reverse transcription PCR (qRT-PCR) (Fig 1C). Compared to the YPD-K cultures, the relative expression levels of Mating type A1 (*MFA1*) (a precursor of *a*-pheromone), *MFA* (a precursor of *α*-pheromone), *STERile 2* (*STE2*) (the *α*-pheromone receptor), and Factor-Induced Gene 1 (*FIG1*) and cell FUSion 1 (*FUS1*) (two pheromone-response genes), as well as *BARI* (an endopeptidase that degrades *α*-pheromone), were all significantly increased in cells grown on YP-K. We also constructed four reporter strains in which *MFA1*, *MFA*, *FIG1*, and *FUS1* were fused with a green fluorescent protein (GFP) fluorescent marker to further confirm their increased expression on YP-K medium (S2 Fig). Thus, glucose depletion leads to the induction of mating-related genes and polarized cell growth, indicative of the development of mating projections in *C. albicans*.

Glucose starvation promotes same-sex mating in *C. albicans*

The induction of both *a*-pheromone and *α*-pheromone precursors in *MTLa/a* cells under glucose-starvation conditions suggests those cells might have lost their original sexual identity, exhibiting features of both *MTLa/a* and *MTLα/α* cells. This, in theory, could bypass the requirement of an *MTLα/α* cell in close proximity to induce homothallic mating between two *MTLa/a* partners. To further explore whether the induction of mating-related genes and polarized cell growth could lead to true homothallic mating, we performed quantitative same-sex mating assays. When two *MTLa/a* strains with different auxotrophic markers (GH1350a and GH1013) were cultured together on YP-K medium, mating projections were observed (Fig 2A), and tetraploid progeny that remained the *a* mating type were generated (Fig 2B and 2C), confirming homothallic mating had occurred. Further, cell fusion between two *MTLa/a* cells and the generation of daughter cells were also observed on YP-K medium (Fig 2A). In contrast, cells remained in yeast form and no mating progeny were isolated when the two *MTLa/a* strains were grown on YPD-K (Fig 2). These results provide the premier example of an environmentally relevant stress, glucose starvation, capable of inducing same-sex mating in *C. albicans*.

Multiple environmental stressors mediate the development of mating projections in *C. albicans*

Glucose deprivation leads to a shift in *C. albicans* metabolism, resulting in the activation of genes involved in the tricarboxylic acid (TCA) cycle and fatty acid β -oxidation [19]. These metabolic changes stimulate the production of reactive oxidative species (ROSs) that cause protein damage, thereby activating the unfolded protein response [22]. The intracellular levels of ROSs in cells of *C. albicans* grown on YP-K medium were significantly higher than those on YPD-K medium and increased with the extension of culture time (Fig 3A). To assess whether

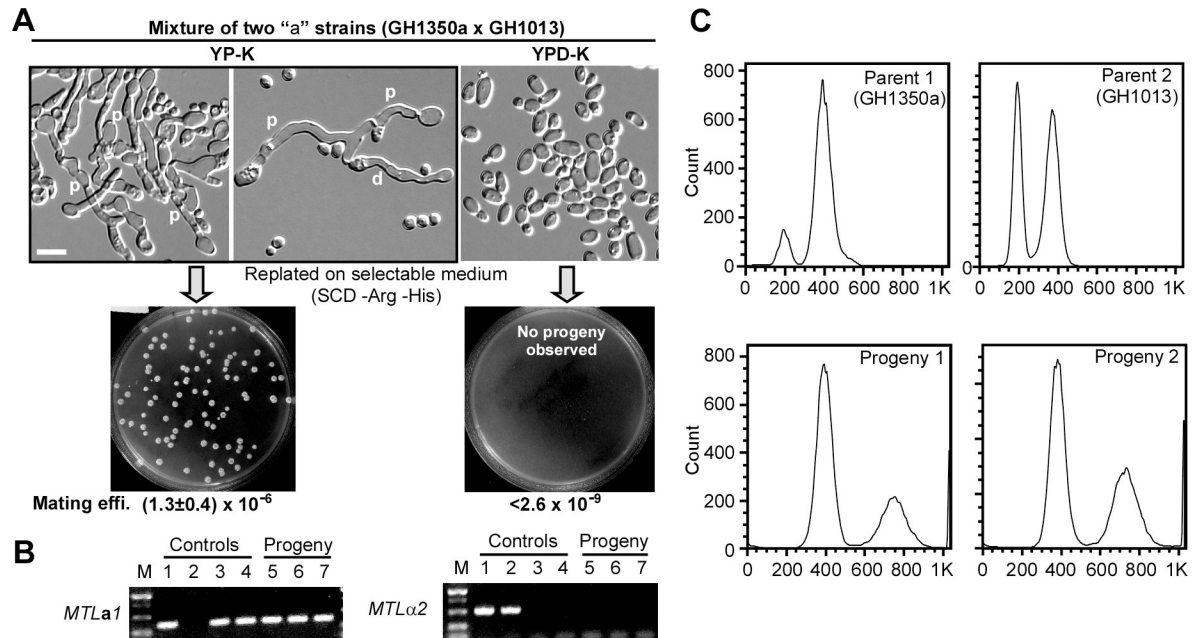


Fig 2. Glucose starvation induces same-sex mating in *C. albicans*. (A) Same-sex mating between two "a" strains (GH1013 and GH1350a). 1×10^7 cells of each strain were mixed and cultured on YPD-K and YP-K media at 25°C. After three days of growth, the mating mixture was replated onto SCD-Arg, SCD-His, and SCD-Arg-His dropout plates to assess mating efficiency. The middle panel (up) indicates that two "a" cells underwent cell fusion and a daughter cell grew out from the conjunction tube. Scale bar, 10 μ m. (B) PCR verification of the *MTL* types. Strains used: lane 1, SN152 (a/a); 2, GH1350 (a/a); 3, GH1350a (a/a); 4, GH1013 (a/a); 5–7, progeny strains of the GH1350a \times GH1013a cross. (C) FACS analysis of the DNA content of parental and progeny strains. Parental diploids have the standard G1 and G2 cell cycle peaks representing 2C and 4C DNA levels. Mating progeny contain DNA content corresponding to 4C and 8C peaks, confirming their tetraploid nature. Arg, arginine; d, daughter cell; FACS, fluorescence-activated cell sorting; His, histidine; M, DNA ladder; *MTL*, Mating type locus; YP-K, yeast extract-peptone- K_2HPO_4 .

<https://doi.org/10.1371/journal.pbio.2006966.g002>

oxidative stress could stimulate homothallic mating, *C. albicans* cells were treated with hydrogen peroxide (H_2O_2), a strong oxidative-stress-inducing agent. Compared to the untreated control, H_2O_2 -treated cells underwent obvious polarized cell development on the glucose-containing medium YPD-K (Fig 3B). Mating-related genes (*MFA1*, *MFA, and *FIG1*) were significantly induced in H_2O_2 -treated cells (Fig 3C), and mating efficiency upon H_2O_2 treatment was comparable to that observed under glucose-deprivation conditions (Fig 3D).*

To further test other environmentally relevant stress conditions, we performed same-sex mating assays using three other nutrient-poor media types: 3% agar with no additional nutrients, agar containing 3% mouse feces, and agar containing *C. albicans* debris. *C. albicans* underwent same-sex mating when cultured on these media types, with mating on mouse-feces-containing medium being most efficient (S3 Fig). Notably, although mating projections morphologically resemble filaments in *C. albicans*, same-sex mating did not occur when cells were cultured on sorbitol medium that induces opaque cell filamentation (S3E Fig). Therefore, multiple nutrient-deprivation conditions are capable of inducing homothallic mating in *C. albicans*.

Glucose starvation induces the expression of mating-related genes, stress-responsive genes, and *HSP90* genetic interactors

To explore the mechanism of glucose-induced same-sex mating in *C. albicans*, we performed global gene-expression-profile analysis. Total RNA was extracted from opaque cells grown on

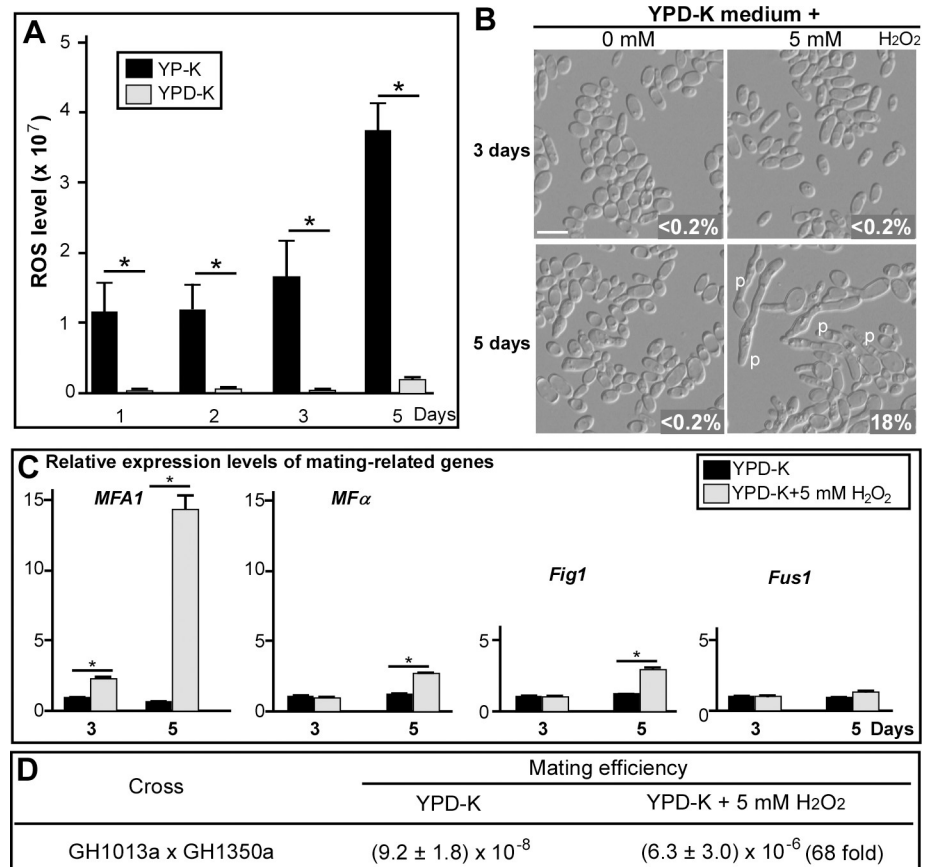


Fig 3. Oxidative stress promotes the development of mating projections in *C. albicans*. (A) Relative ROS levels. 1×10^5 cells of strain GH1013 were spotted on YPD-K and YP-K media and cultured at 25°C for one, two, three, or five days. For each day, 1×10^6 cells were used for ROS level determination. Error bars represent standard deviation of three biological replicates. * indicates significant difference ($p < 0.05$, two-tailed Student *t* test). (B) H₂O₂ induces the development of mating projections in the presence of glucose. 200 μ L of H₂O or 5 mM H₂O₂ solution was spread on YPD-K medium plates (90 mm). 1×10^6 cells of strain GH1350a were spotted on the medium and cultured at 25°C for three or five days. Percentages of projected cells are indicated in the corresponding images. (C) Relative expression levels of mating-related genes in response to H₂O₂ treatments on YPD-K medium. Error bars, standard errors of technical duplicates. * $p < 0.05$, two-tailed Student *t* test. Experiment was performed in biological replicate, and a representative image is shown. (D) Efficiency of same-sex mating on YPD-K medium with or without H₂O₂ treatment. The mating mixtures were grown on different media at 25°C for seven days. To make YPD-K + H₂O₂ plates, 200 μ L H₂O₂ (5 mM) was spread on the medium surface (of a 90-mm plate). The numerical data are presented in [S3 Data](#). FIG1, Factor-Induced Gene 1; FUS1, cell FUSion 1; MFA1, Mating type A1; MF α , Mating α factor precursor; p, mating projection; ROS, reactive oxidative species; YPD-K, yeast extract-peptone-glucose-K₂HPO₄; YP-K, yeast extract-peptone-K₂HPO₄.

<https://doi.org/10.1371/journal.pbio.2006966.g003>

YPD-K or YP-K media at 25°C for 60 hours, and the samples collected were used for RNA sequencing (RNA-Seq) assays. We incubated cells for only 60 hours because mating projections were not induced at this time point, enabling us to minimize indirect effects on gene expression. As demonstrated in [Fig 4](#) and [S1 Data](#), we found 412 genes up-regulated in YPD-K medium and 408 genes up-regulated in YP-K medium (with a change greater than 1.5-fold). As expected, a number of mating-related genes—including *MFA1*, *BAR1*, *Candida* ERK-family protein kinase (*CEK1*), and *CEK2*—were up-regulated in YP-K medium. Heat-shock-protein-encoding genes and oxidative-stress-responsive genes were also up-regulated in YP-K medium, whereas cell-wall-related and glycosylphosphatidylinositol (GPI)-anchored protein-encoding genes were enriched in YPD-K medium. Of the differentially expressed

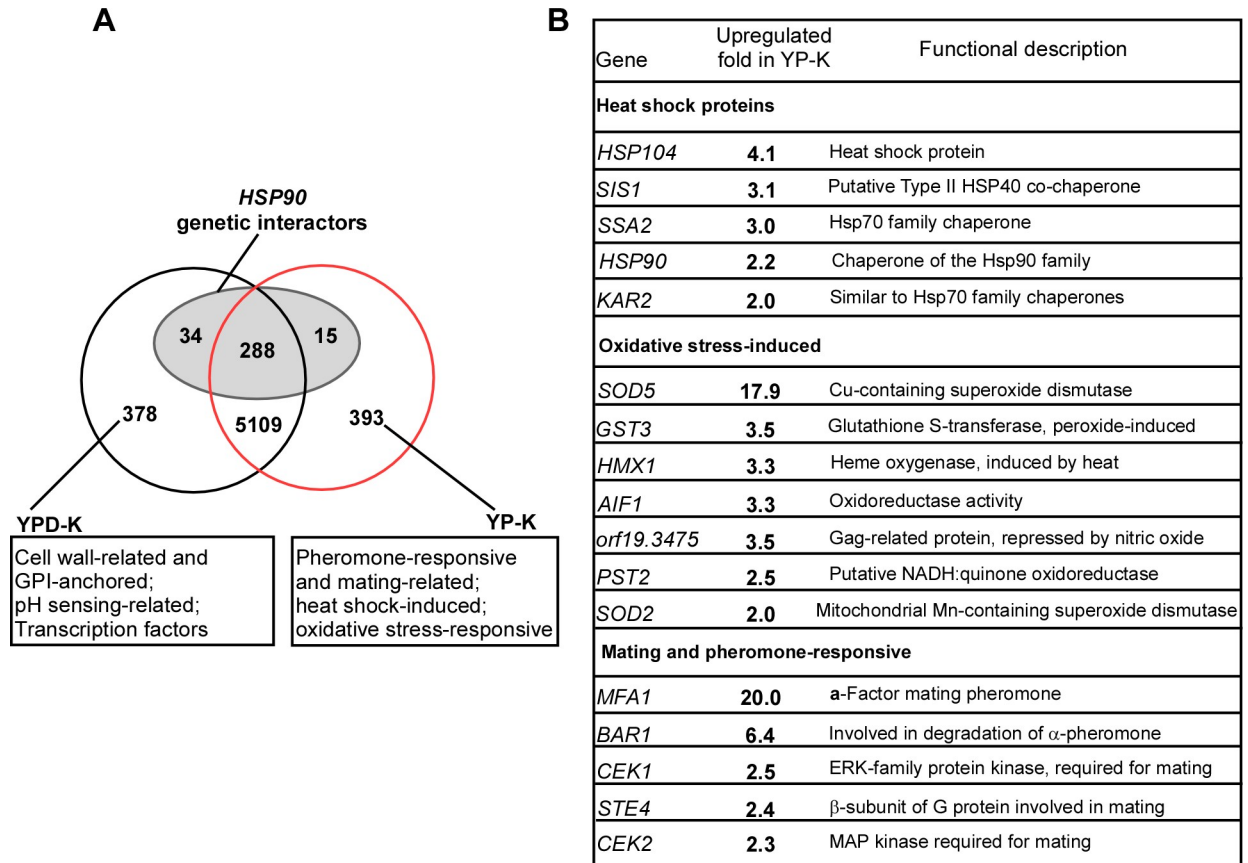


Fig 4. Global gene-expression-profile analysis of *C. albicans* in the presence and absence of glucose. *C. albicans* cells were spotted and grown on YPD-K or YP-K media at 25°C for 60 hours. Total RNA was extracted and used for RNA-Seq assays. To be considered differentially expressed, a gene must satisfy three criteria: (1) an FPKM value higher than or equal to 20 at least in one sample, (2) a fold change value higher than or equal to 1.5, and (3) an adjusted *p*-value (FDR) lower than 0.05. (A) Venn diagram depicting relationships between differentially expressed genes on YPD-K (412) and YP-K (408) media and *HSP90* genetic interactors (indicated in the ellipse). (B) Selected heat-shock-protein-encoding, oxidative-stress-induced, and mating-related genes up-regulated in YP-K medium. *AIF1*, Apoptosis-Inducing Factor 1; *BAR1*, BARrier 1; *CEK1*, *Candida* ERK-family protein kinase; ERK, ERK-family protein kinase; FDR, false discovery rate; FPKM, fragments per kb per million reads; GPI, glycosylphosphatidylinositol; *GST3*, Glutathione S-transferase; *HMX1*, HeMe oXygenase; *Hsp90*, Heat shock protein 90; *KAR2*, KARyogamy; MAP, mitogen-activated protein; *MFA1*, Mating type A1; NADH, Nicotinamide adenine dinucleotide; *orf19.3475*, *Candida* gene *orf19.3475*; *PST2*, Protoplasts-SecTed 1; RNA-Seq, RNA sequencing; *SIS1*, Slt4 Suppressor; *SOD5*, SuperOxide Dismutase 5; *SSA2*, Stress-Seventy subfamily A; *STE4*, STERile 4; YPD-K, yeast extract-peptone-glucose-K₂HPO₄; YP-K, yeast extract-peptone-K₂HPO₄.

<https://doi.org/10.1371/journal.pbio.2006966.g004>

genes, 49 have been reported as *HSP90* genetic interactors (Fig 4A and S2 Data) [23, 24]. Among the differentially expressed *HSP90* genetic interactors, 34 genes were down-regulated and only 15 genes were up-regulated in YP-K medium. These genes were enriched in gene functions associated with stress response, cell wall, transcriptional regulation, and signaling transduction.

Down-regulation of Hsf1–Hsp90 signaling promotes mating-projection formation and same-sex mating

Several observations led us to hypothesize that Hsp90 could play an important role in the regulation of glucose-starvation-induced mating-projection formation and same-sex mating. First, glucose starvation increased the intracellular level of ROSs (Fig 3A) that would contribute to increased protein damage, thus likely overwhelming the functional capacity of Hsp90. Second, the treatment of oxidative reagents (e.g., H₂O₂) that led to the increase of intracellular ROSs

induced mating-projection formation and same-sex mating in *C. albicans* (Fig 3B, 3C and 3D). Third, a number of heat-shock-protein-encoding genes, including *HSP90*, were up-regulated in the absence of glucose, further suggesting that Hsp90 functional capacity was overwhelmed (Fig 4B and S1 Data).

The conserved heat-shock transcription factor Hsf1 plays an important role in regulating the expression of heat-shock proteins, including the molecular chaperone Hsp90 in *C. albicans* and other eukaryotes [25, 26]. Hsf1 has been implicated in regulating transcriptional changes in response to oxidative stresses and glucose starvation in *S. cerevisiae* [27, 28]. Therefore, we first tested the role of Hsf1 in the development of mating projection and homothallic mating in *C. albicans*. Since Hsf1 is essential for cell viability, we generated a tetracycline-induced (*tetON*)-promoter-controlled conditional expression mutant, *tetON-HSF1/hsf1*, in order to assess how changes in Hsf1 levels influence same-sex mating. In the absence or presence of 40 $\mu\text{g}/\text{mL}$ doxycycline, the *tetON-HSF1/hsf1* mutant formed wrinkled colonies and underwent robust polarized growth on YP-K medium (Fig 5A). Of note, doxycycline (40 $\mu\text{g}/\text{mL}$) exhibited an inhibitory effect on the induction of mating projection formation in the wild-type (WT) control (Fig 5A). With increased exposure to glucose on YPD-K medium, mating projections were only observed in the absence of doxycycline after five days but not upon the addition of 40 $\mu\text{g}/\text{mL}$ doxycycline nor in the WT control (Fig 5A).

Consistent with the morphological changes, mating-related genes—including *MFA1*, *MFA α* , *FIG1*, and *FUS1*—were induced in the *tetON-HSF1/hsf1* mutant on both YP-K and YPD-K media relative to the WT strain (Fig 5B). Finally, we tested the effect of *HSF1* depletion on homothallic mating. In the absence of doxycycline, the *tetON-HSF1/hsf1* mutant underwent same-sex mating with the WT partner even on the glucose-containing YPD-K medium, albeit at a lower frequency than that observed in glucose-limiting conditions (S1 Table and S4 Fig). However, in the presence of 40 $\mu\text{g}/\text{mL}$ doxycycline, neither the *tetON-HSF1/hsf1* mutant nor the WT control could undergo homothallic mating on YPD-K medium. Taken together, our results indicate that down-regulation of Hsf1 promotes mating-projection formation and same-sex mating in *C. albicans*, bypassing the requirement of glucose starvation.

Next, we wanted to evaluate whether the impact of Hsf1 on homothallic mating might be mediated through its regulatory effects on *HSP90*. We constructed a *tetON-HSP90/hsp90* strain using an analogous *tetON*-promoter-controlled conditional expression strategy. As shown in Fig 6, culturing this strain in media containing 40 $\mu\text{g}/\text{mL}$ doxycycline was required to bypass a substantial growth defect of the strain. Further, opaque cells of the conditional *tetON-HSP90/hsp90* strain were not stable, and therefore an *ACT1* promoter controlling White-Opaque Regulator 1 (*WOR1*), the master regulator of the opaque phenotype, was introduced in the mutant to maintain the opaque state. Similar to the *tetON-HSF1/hsf1* mutant, the *tetON-HSP90/hsp90* strain underwent the development of mating projections on both YP-K and YPD-K media containing 40 $\mu\text{g}/\text{mL}$ doxycycline (Fig 6A). However, the WT control was unable to form mating projections under the same culture conditions (Fig 6A). In the presence of 100 $\mu\text{g}/\text{mL}$ doxycycline, the ratio of projected cells on YPD-K medium was remarkably reduced (Fig 6A). As expected, mating-related genes *FIG1* and *FUS1* were induced on YP-K medium, while *MFA1* and *MFA α* were induced in the *tetON-HSP90/hsp90* mutant on both media relative to the WT strain in the presence of 40 $\mu\text{g}/\text{mL}$ doxycycline (Fig 6B). As demonstrated in S4A Fig, the relative transcript levels of *HSF1* or *HSP90* in the *tetON-HSF1/hsf1* or *tetON-HSP90/hsp90* mutant were lower than that in the WT strain even in the presence of 40 $\mu\text{g}/\text{mL}$ doxycycline. Together, these data suggest that reduction of *HSF1* or *HSP90* levels leads to the induction of a homothallic mating program and bypasses the requirement for glucose depletion.

Transcription factors Cta4 and Cwt1 regulate the development of mating projections and same-sex mating

To further characterize the regulatory mechanism of glucose starvation-induced mating, we screened a transcription factor homozygous deletion library (in an *MTLa/a* background) [29]

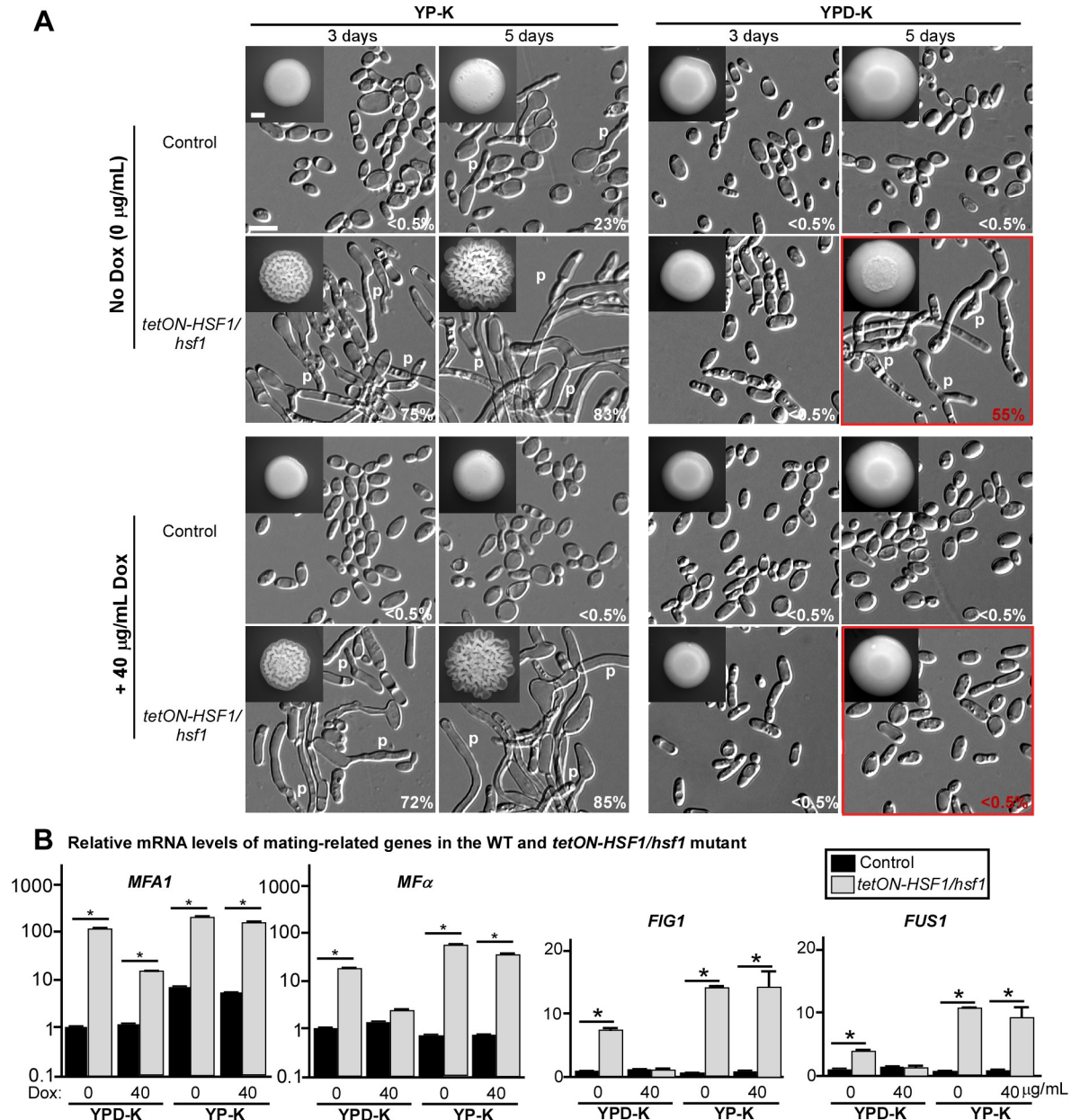


Fig 5. Role of Hsf1 in the induction of mating projections in *C. albicans*. (A) Morphologies of the control and *tetON-HSF1/hsf1* mutant. 1×10^5 cells were spotted on YPD-K and YP-K media without or with 40 µg/mL Dox and cultured at 25°C for three or five days. Percentages of projected cells are indicated in the corresponding images. Scale bar for colonies, 2 mm (inset); scale bar for cells, 10 µm. Control, GH1013cartTA. (B) Relative expression levels of mating-related genes. 1×10^5 cells of each strain were cultured on YPD-K medium (for six days) or on YP-K medium (for three days) without or with 40 µg/mL Dox at 25°C. Error bars represent standard errors of technical duplicates. * $p < 0.05$, two-tailed Student *t* test. Experiment was repeated in a biological replicate, and a representative image is shown. The numerical data are presented in S3 Data. Dox, doxycycline; *FIG1*, Factor-Induced Gene 1; *FUS1*, cell FUSion 1; Hsf1, Heat Shock transcription Factor 1; *MFA1*, Mating type A1; *MFAα*, Mating α factor precursor; p, mating projection; *tetON*, tetracycline-induced; *tetON-HSF1/hsf1*, *tetON*-promoter-controlled conditional expression strain of *HSF1*; WT, wild type; YPD-K, yeast extract-peptone-glucose-K₂HPO₄; YP-K, yeast extract-peptone-K₂HPO₄.

<https://doi.org/10.1371/journal.pbio.2006966.g005>

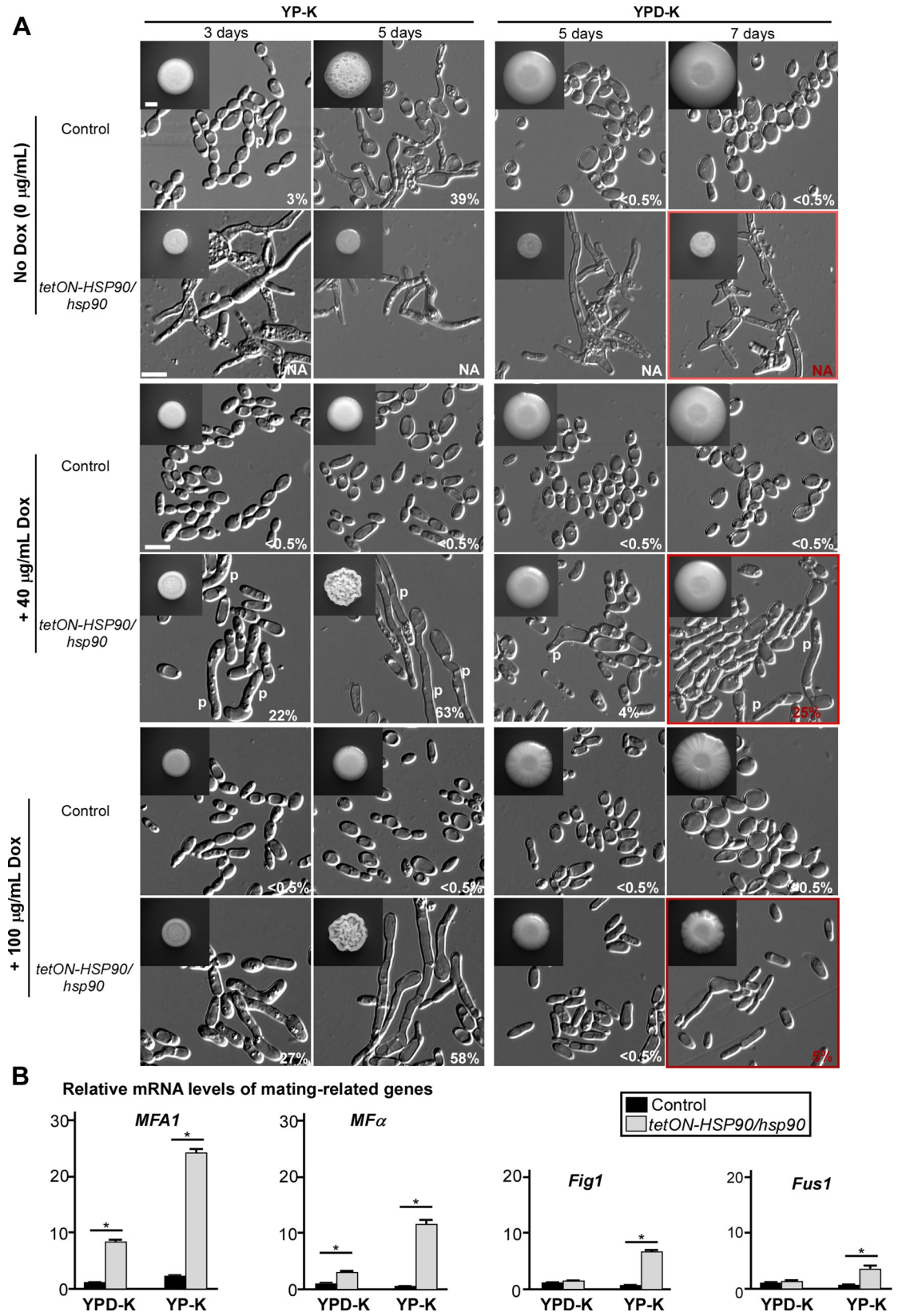


Fig 6. Down-regulation of Hsp90 promotes the development of mating projections. (A) Morphologies of the control and *tetON-HSP90/hsp90* mutant. Control, GH1013 + pACT1-WOR1; *tetON-HSP90/hsp90*, a *tetON*-promoter-controlled conditional expression strain of HSP90 with ectopically expressed WOR1 (+ pACT1-WOR1). 1×10^5 cells were spotted on YPD-K and YP-K media with or without Dox as indicated and cultured at 25°C for three, five, or seven days. Percentages of projected cells are indicated in the corresponding images. Scale bar for colonies, 2 mm (inset); scale bar for cells, 10 μ m. (B) Relative expression of mating-related genes. 1×10^5 cells of each strain were cultured on YPD-K medium (for seven days) or on YP-K medium (for three days) with 40 μ g/mL Dox at 25°C. Relative expression levels were not tested on YP-K medium without Dox since cell viability of the *tetON-HSP90/hsp90* mutant was severely impaired. Error bars represent standard errors of technical duplicates. * $p < 0.05$, two-tailed Student *t* test. Experiment was repeated in a biological replicate, and a representative image is shown. The numerical data are presented in **S3 Data**. Dox, doxycycline; FIG1, Factor-Induced Gene 1; FUS1, cell FUSion 1; Hsp90, Heat shock protein 90; MFA1, Mating type A1; MF α , Mating α factor precursor; NA, not analyzed; p, mating projection; pACT1, plasmid pACT1; *tetON*, tetracycline-induced; WOR1, White-Opaque Regulator 1; YPD-K, yeast extract-peptone-glucose-K₂HPO₄; YP-K, yeast extract-peptone-K₂HPO₄.

<https://doi.org/10.1371/journal.pbio.2006966.g006>

to look for mutants capable of enhanced mating projection formation. Through this functional genomic screening approach, we identified the transcription factors Cwt1 and Cta4 that function as negative and positive regulators of the development of mating projections in *C. albicans*, respectively (**S5 Fig** and **S6 Fig**). Homozygous deletion of *CWT1*, a gene involved in the nitrosative stress response [30], resulted in an increase in mating-projection formation on YP-K medium at three days compared to the WT control. Unlike the WT control that grew exclusively as yeast on YPD-K, *cwt1/cwt1* mutants also showed polarized growth (**S5A Fig**). As expected, mating-related genes *MFA1*, *MF α* , *FIG1*, and *FUS1* were significantly increased in the *cwt1/cwt1* mutant on YPD-K relative to a WT control (**S5B Fig**). To verify the function of Cwt1 in regulating homothallic mating, we generated an additional homozygous *CWT1* deletion mutant in the GH1013 background. Similar to the library mutant, the newly generated *cwt1/cwt1* strain exhibited a more robust development of mating projections on both YP-K and YPD-K than the WT control (**Fig 7A and 7B**), and also promoted same-sex mating on YPD-K medium (**S1 Table**). Thus, Cwt1 represses homothallic mating in *C. albicans*.

In contrast, deletion of *CTA4*, a previously identified genetic interactor of Hsp90 [23, 24] and a gene induced by nitric oxide, significantly repressed the development of mating projections in YP-K medium in *C. albicans* (**S6A Fig**). Consistently, the expression of mating-related genes was not induced in the *cta4/cta4* mutant in YP-K medium, unlike in the WT control (**S6B Fig**). However, the relative expression levels of *CWT1* were significantly increased in the *cta4/cta4* mutant, and chromatin immunoprecipitation (ChIP) assays demonstrated that Cta4 bound to the promoter regions of *CWT1* on YP-K medium (**S6C Fig**). Thus, Cta4 may provide a functional connection between Hsp90 and Cwt1 and directly regulate the transcriptional expression of *CWT1*.

Consistently, we found that the transcription level of *CWT1* was down-regulated in YP-K medium compared to the level observed in YPD-K medium (**Fig 7C**). Moreover, in the *tetON-HSF1/hsf1* background in which levels of *HSF1* were reduced relative to a WT control, we also observed a significant reduction in *CWT1* transcript levels (**Fig 7D**), suggesting that the transcriptional expression of *CWT1* is directly or indirectly regulated by Hsf1–Hsp90 signaling.

Protein sequence analysis indicated that Cwt1 contains a Zn₂Cys₆ motif at the carboxyl terminus and a conserved Per-Arnt-Sim (PAS) domain at the amino terminus. Since the PAS domain often interacts with Hsp90 in eukaryotic organisms [31, 32], we next tested whether Hsp90 was able to bind to Cwt1 and regulate its activity in *C. albicans*. As shown in **Fig 7E**, co-immunoprecipitation (IP) assays indicated that Hsp90 and Cwt1 physically interact on YP-K, but not YPD-K, medium. Therefore, Hsf1–Hsp90 signaling may regulate the activity of Cwt1 at post-transcriptional levels as well as at the transcriptional level via Cta4 in *C. albicans*.

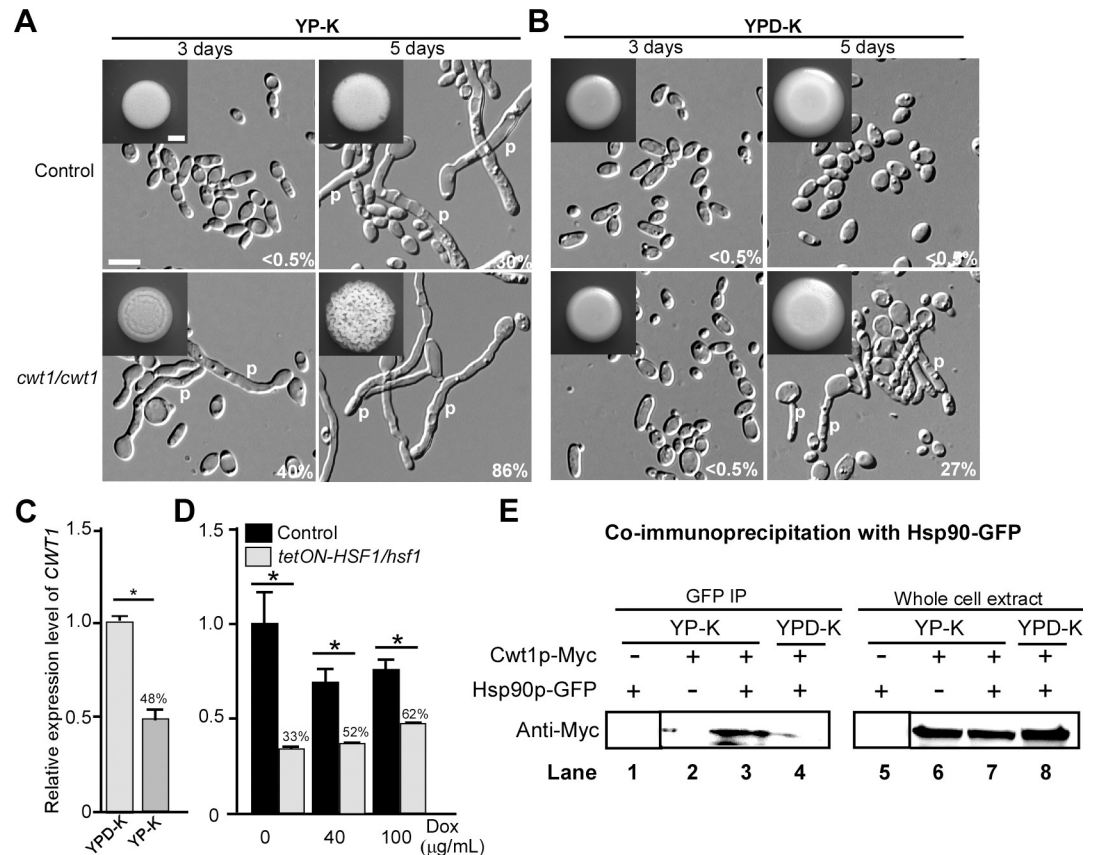


Fig 7. Role of the Cwt1 transcription factor in the induction of mating projections. (A and B) Morphologies of the control (GH1013 + ARG4 + HIS1) and *cwt1/cwt1* mutant on YP-K (A) or YPD-K (B) medium. 1×10^5 cells of each strain were spotted on YPD-K and YP-K media and cultured at 25°C for three or five days. Percentages of projected cells are indicated in the corresponding images. Scale bar for colonies, 2 mm (inset); scale bar for cells, 10 μ m. (C) Relative expression levels of CWT1 in YPD-K and YP-K media. Cells of *C. albicans* were spotted on YPD-K and YP-K media and cultured at 25°C for five days. (D) Relative expression levels of CWT1 in the control (GH1013cartTA) and *tetON-HSF1/hsf1* on YP-K medium. Error bars, standard errors of technical duplicates. * $p < 0.05$, two-tailed Student *t* test. Percentages indicate the ratio of gene expression in *tetON-HSF1/hsf1* mutant relative to gene expression in control. The numerical data are presented in S3 Data. (E) Physical interaction of Cwt1 and Hsp90. Co-IP assays were performed using a strain with 13 \times Myc-tagged Cwt1 and GFP-tagged Hsp90. Lanes 1–4, samples co-immunoprecipitated by the GFP antibody Sepharose and analyzed by immunoblotting with the anti-Myc antibody. Lanes 5–8, whole-cell extracts analyzed by immunoblotting with the anti-Myc antibody. Experiment was performed in biological replicate, and a representative image is shown. Arg, arginine; Cwt1, Cell Wall Transcription factor 1; Dox, doxycycline; GFP, green fluorescent protein; His, histidine; Hsf1, Heat Shock transcription Factor 1; Hsp90, Heat shock protein 90; IP, immunoprecipitation; Myc, Myc epitope tag; p, mating projection; *tetON*, tetracycline-induced; *tetON-HSF1/hsf1*, *tetON*-promoter-controlled conditional expression strain of *HSF1*; YPD-K, yeast extract-peptone-glucose-K₂HPO₄; YP-K, yeast extract-peptone-K₂HPO₄.

<https://doi.org/10.1371/journal.pbio.2006966.g007>

Cwt1 regulates the master regulator of a-type mating, MTLa2, to control same-sex mating

MTLa2 is required for the maintenance of a-cell identity [33]. Inactivation of MTLa2 induces the expression of α -pheromone in MTLa/a cells of *C. albicans* [33]. Given our observation that glucose starvation induced the expression of both pheromone precursors MFA1 and MF α , we assessed whether homothallic mating induced in glucose-limiting conditions was governed by changes in MTLa2 levels. To test this, we overexpressed MTLa2 and observed a suppression in the development of mating projections under glucose-limiting conditions (Fig 8A and 8B). Next, to test whether compromise of Hsf1–Hsp90–Cwt1 signaling impaired MTLa2 expression, we monitored MTLa2 levels in our *tetON-HSF1/hsf1* and *tetON-HSP90/hsp90* mutants.

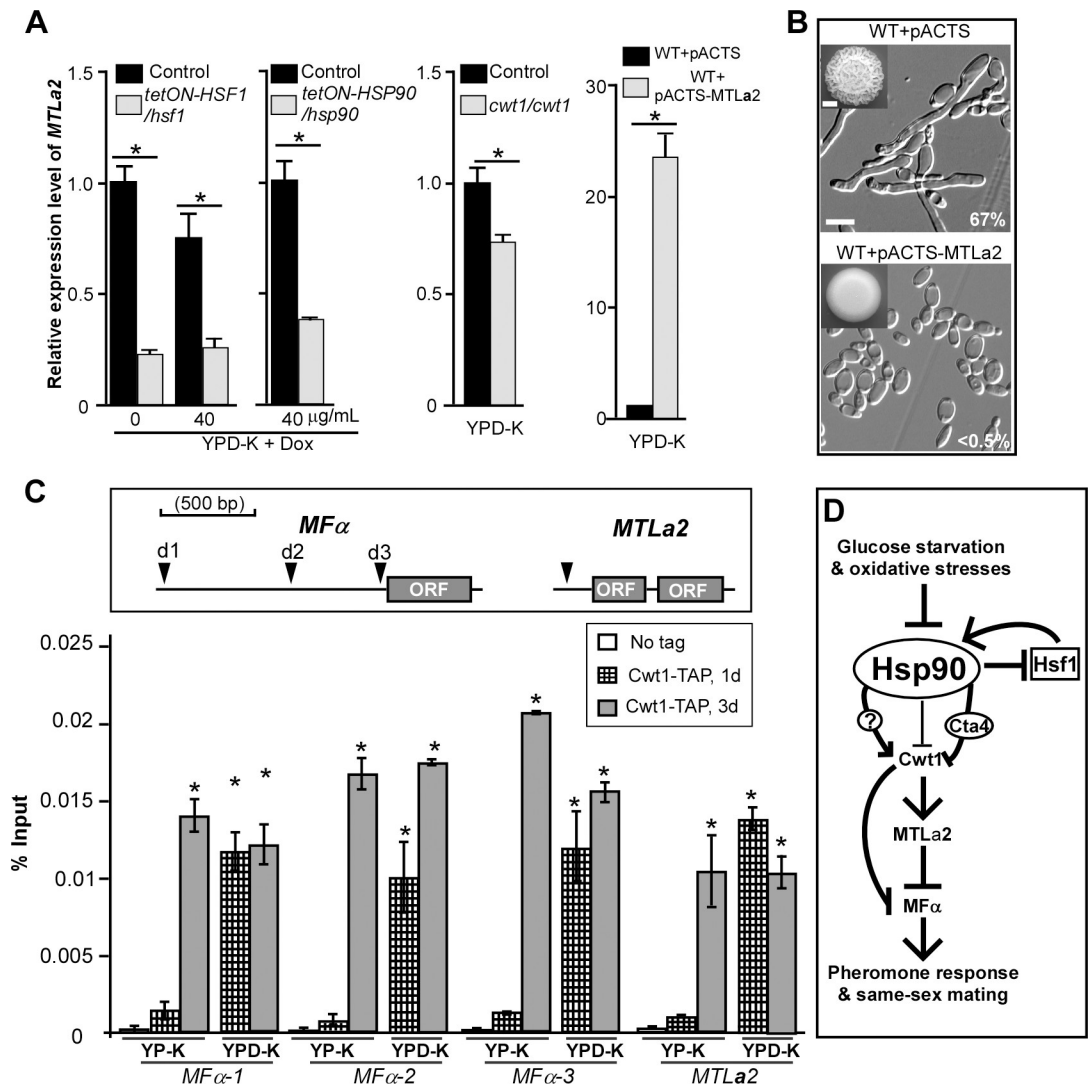


Fig 8. *MTLa2* regulates the development of mating projections in *C. albicans*. (A) Relative expression levels of *MTLa2* in the corresponding controls, *tetON-HSF1/hsf1*, *tetON-HSP90/hsp90*, and *cwt1/cwt1* mutants, and *MTLa2*-overexpressing strain on YPD-K medium. Transcript levels were normalized to *ACT1*. Error bars, standard errors of technical duplicates. **p* < 0.05, two-tailed Student *t* test. Experiment was performed in biological replicate, and a representative image is shown. (B) 1×10^5 cells of each strain were spotted on YP-K medium and cultured at 25°C for five days. Morphologies of the control (WT + pACTS) and *MTLa2*-overexpressing strains (WT + pACTS-*MTLa2*) on YP-K medium. WT, GH1350a. Scale bar for colonies, 2 mm (inset); scale bar for cells, 10 μm. (C) Cwt1 binds to the promoters of *MTLa2* and *MFα*. ChIP assays were performed in TAP-tagged Cwt1 strains. Percentages of input genomic DNA are indicated. 1×10^5 cells of each strain were spotted on YP-K or YPD-K media and cultured at 25°C for one or three days. Dark arrows indicate detected promoter regions. d1, d2, and d3, three detected sites of *MFα*. Error bars represent standard error of two technical replicates. **p* < 0.05, two-tailed Student *t* test. Experiment was performed in biological replicate with a representative image shown. The data for the untagged control correspond to samples harvested at day 1. The numerical data are presented in S3 Data. (D) Regulatory model of glucose-starvation- or oxidative-stress-induced same-sex mating in *C. albicans*. Glucose starvation or oxidative stresses cause the overwhelming of the Hsf1/Hsp90 functional capacity that regulates the transcriptional expression and activity of *CWT1* in both direct and indirect manners. Cwt1 regulates same-sex mating through the control of *MFα* or *MTLa2*. *ACT1*, *ACT1n* 1; ChIP, chromatin immunoprecipitation; Cta4, *Candida* TransActivating protein 4; Cwt1, Cell Wall Transcription factor 1; Dox, doxycycline; Hsf1, Heat Shock transcription Factor 1; Hsp90, Heat shock protein 90; *MFα*, Mating α factor precursor; *MTL*, Mating type locus; pACTS, plasmid pACTS; TAP, Tandem affinity purification; *tetON-HSF1/hsf1*, *tetON*-promoter-controlled conditional expression strain of *HSF1*; WT, wild type; YPD-K, yeast extract-peptone-glucose-K₂HPO₄; YP-K, yeast extract-peptone-K₂HPO₄.

<https://doi.org/10.1371/journal.pbio.2006966.g008>

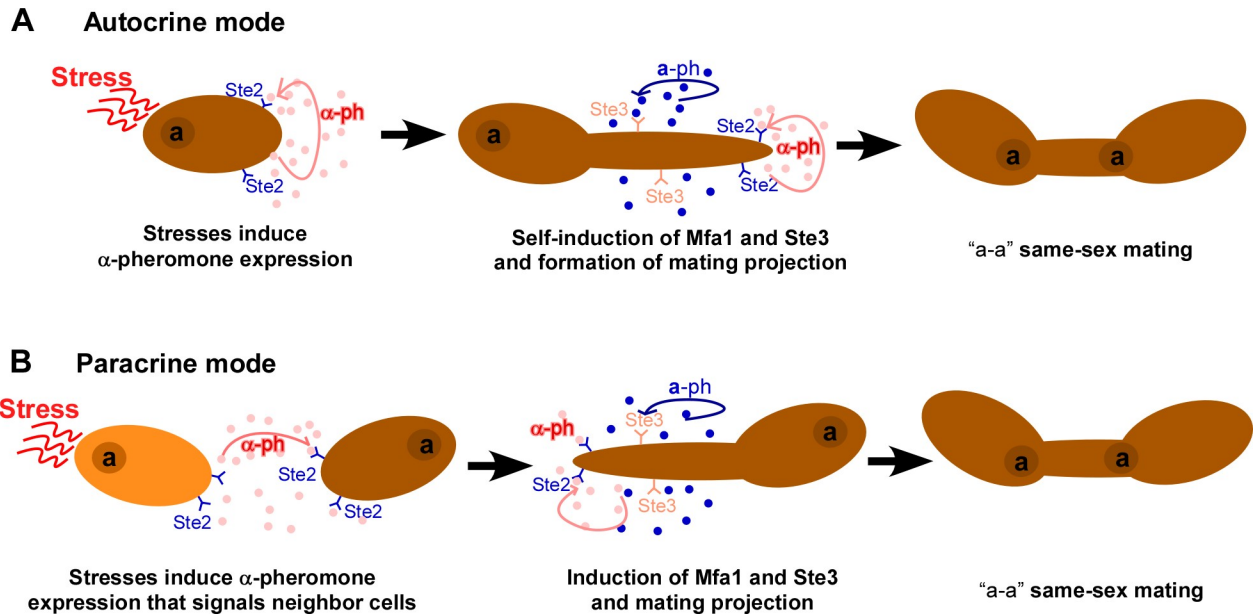


Fig 9. Potential autocrine (A) and paracrine (B) pheromone response models for stress-induced mating-projection formation and same-sex mating. Neither α -pheromone nor a-pheromone is constitutively expressed in "a" cells of *C. albicans*. Glucose starvation or oxidative stress first induces α -pheromone and its receptor Ste2 expression in "a" cells. α -pheromone binds to Ste2 and activates the pheromone-response pathway, which subsequently induces the expression of a-pheromone. "a" cells then become mating competent as both "a" and " α " types. The activation of the pheromone-response pathway promotes mating projection formation and same-sex mating. Autocrine pheromone response, self-activation (A); paracrine pheromone response, activation of neighbor cells (B). *MFA1*, Mating type A1; *STE2*, *STERile 2*.

<https://doi.org/10.1371/journal.pbio.2006966.g009>

Down-regulation of *HSF1* or *HSP90* or deletion of *CWT1* led to significantly decreased expression of *MTLa2* on YPD-K medium (Fig 8A), implicating this stress-response signaling in the regulation of *MTLa2* expression. It has been indicated that Cwt1 has potential binding sites in the promoter regions of *MTLa2* and *MFA* genes [34]. Using ChIP assays, we observed that Cwt1 directly binds to the promoter regions of both *MTLa2* and *MFA* on YPD-K medium in the one-day cultures, and this binding activity was observed on both on YP-K and YPD-K media in the three-day cultures (Fig 8C). These results suggest that Cwt1 directly regulates mating-related gene expression.

Overall, our data suggest a model in which Hsf1–Hsp90 signaling controls the expression of Cwt1 through Hsp90 genetic interactors such as Cta4 as well as the activity of Cwt1 post-translationally through a physical interaction with Hsp90. Cwt1 is a dimeric Zn₂Cys₆ zinc-finger transcription factor. The physical interaction between Hsp90 and Cwt1 could inhibit the dimerization of Cwt1 through the PAS domain in *C. albicans*, as observed in other eukaryotic organisms [32]. Cwt1 binds to the promoters of *MFA* or *MTLa2* and regulates their transcriptional expression (Fig 8D). It has been demonstrated that same-sex mating in *C. albicans* is induced by the autocrine and/or paracrine pheromone response [16]. Therefore, the activated pheromone signaling by the environmental cues could then promote the development of mating projections and same-sex mating, possibly through these two response modes (Fig 9).

Discussion

The predominantly clonal nature of *C. albicans* greatly limits the occurrence of heterothallic mating between two competent cells with opposite mating types in its natural environment. It would be difficult for a mating-competent cell of *C. albicans* to find a competent cell with an opposite mating type to mate. Although the efficiency of same-sex mating is much lower than

that of opposite-sex mating under laboratory conditions in *C. albicans* [16], same-sex mating involving cells of a single type would lower the barrier to finding a suitable partner [35]. However, the requirement of α -pheromone production in close proximity to drive homothallic mating between two *MTLa* cells or the need to inactivate the Bar1 protease challenges the relevance of same-sex mating in nature [16]. This is especially true given that neither natural *C. albicans* mutants with loss of Bar1 function nor environmental conditions suppressing Bar1 activity have been discovered. Thus, the question remains: can *C. albicans* undergo frequent same-sex mating in natural environments?

In our current study, we find that glucose starvation and oxidative stress induce same-sex mating in *MTLa* cells of *C. albicans*, providing an environmentally relevant means to drive sexual reproduction in this species. *C. albicans* is commonly exposed to glucose starvation because glucose is limited in its natural niches such as the mouth, lower gut, and environments contaminated with human or animal excreta. However, under the same conditions, we did not observe same-sex mating in opaque Mating type α (*MAT α*) cells, perhaps because of *MTLa2*, a key regulator in this induction in *MTLa* cells. *MAT α / α* cells may use a different environmental cue for the induction of same-sex mating. Similar to reports highlighting that the fungal pathogen *Cryptococcus neoformans* undergoes mating on pigeon guano [36], we found that animal feces promoted same-sex mating in *C. albicans* (S3 Fig). Given that the gut of human or warm-blooded animals is a major natural niche for *C. albicans* [12], animal feces would be a major source for most nutritional components. Furthermore, growth on *C. albicans* debris medium containing no additional nutrients also induced same-sex mating (S3 Fig). When yeast grows on agar-only medium, a portion of cells undergo cell death and release nutrients for the growth and survival of neighboring cells [37]. Under these glucose-limiting conditions, the frequency of same-sex mating in *C. albicans* ranged from 1×10^{-7} to 3×10^{-5} (S3 Fig), suggesting that the average-aged colony (containing approximately 1×10^8 cells) can produce tens to hundreds of mating progeny. Therefore, the occurrence of same-sex mating under glucose starvation conditions could be considerably more frequent in nature than was originally thought.

The notion that environmental stress may serve as a trigger to induce more frequent sexual reproduction in *C. albicans* has been previously proposed based on a series of observations [38]. Poor nutritional conditions increase the frequency of opposite-sex mating [39]. Oxidative stress promotes the induction of the white-to-opaque switch [40], and recombination occurs more frequently following exposure to several types of stress, which would provide a critical step for the homozygosis of the *MTL* locus. Despite these lines of evidence, our work provides the seminal example of stressful conditions governing homothallic mating in *C. albicans*. In *C. neoformans*, sexual mating is stimulated by stresses such as nitrogen starvation, desiccation, and darkness [41]. Moreover, treatment of *S. pombe* with the oxidative agent H_2O_2 promotes the generation of meiotic spores [42]. Therefore, exposure to harsh environmental conditions could be a general signal for diverse fungal species to integrate environmental response pathways with increased sexual reproduction.

The evolutionarily conserved regulators Hsf1 and Hsp90 play a primary and global role in orchestrating stress responses in eukaryotic organisms [43]. Glucose starvation results in the production of ROSs (Fig 3) that would likely cause protein damage in *C. albicans*. Under these situations, the functional capacity of Hsp90 could be overwhelmed, causing it to be titrated away from its basal client proteins while it deals with more global problems of protein misfolding. Consistently, a number of heat-shock-protein-encoding genes, including *HSP90*, were up-regulated in response to glucose deprivation (Fig 4 and S1 Data).

In our study, we implicate the Cta4 and Cwt1 transcription factors, which regulate the nitrosative or nitric oxide stress response [30], as downstream effectors of the Hsf1–Hsp90

signaling and mating-response pathways (Fig 8). Cta4 has been previously reported as a genetic interactor of Hsp90 [23, 24] and represses the transcriptional expression of *CWT1*. Moreover, we demonstrate that Hsp90 directly binds to Cwt1 on YP-K but not YPD-K medium, perhaps through the conserved PAS motif of Cwt1. To our knowledge, this is the first time that Hsf1 or Hsp90 have been implicated in sexual mating in fungi, and our results suggest that diverse cellular stresses capable of overwhelming the function of these regulators, including elevated temperature, may also promote sexual reproduction in *C. albicans*.

Inactivation of the Bar1 protease or the Dipeptidyl aminopeptidase YC1 (Yci1) domain protein Opaque Formation Regulator 1 (Ofr1) has been shown to induce same-sex mating in *C. albicans* [16, 44]. We observed that *BARI* was not down-regulated but rather highly induced upon glucose starvation (Fig 1). Further, inactivation of Ofr1 allows *MTLa/a* cells to undergo same-sex mating as the “a” mating type [44]. Although glucose starvation can only induce same-sex mating in *MTLa/a* cells but not in *MTLa/a* or *MTLa/a* cells, other unidentified environmental conditions may allow *MTLa/a* or *MTLa/a* cells to undergo homothallic mating. Therefore, glucose-starvation-induced same-sex mating appears to be independent of Bar1 and Ofr1.

In summary, we uncover a novel, to our knowledge, environmental trigger, glucose depletion, capable of acting as a signal for sexual mating in *C. albicans*, which not only sheds light on the biology of this pathogen but also expands the diverse repertoire of sexual reproduction modes in fungi. This strategy is different from that used by *S. cerevisiae*, *S. pombe*, and *C. neoformans*, despite the fact that the evolutionarily diverse yeast species achieve a same output for homothallicism. Unisexual reproduction generates aneuploidy and de novo phenotypic diversity in fungi [45, 46], thus providing a selective advantage under stressful conditions over those organisms propagating exclusively in an asexual manner. *C. albicans* exists as an obligate diploid in nature, with many heterozygous loci between homologous chromosomes. Therefore, when tetraploid intermediate cells generated from same-sex mating return to a lower ploidy state, there is substantial opportunity for the generation of genetically diverse progeny. These tetraploid strains could serve as a capacitor for generating distinct aneuploidies and randomly combined chromosome sets in order to facilitate the evolution of new traits to adapt to changing environments.

Materials and methods

Strains and culture conditions

The strains used in this study are listed in supplementary S2 Table. YPD (20 g/L peptone, 10 g/L yeast extract, 20 g/L glucose) and modified Lee's glucose medium supplemented with 5 µg/ml phloxine B [47] were used for routine growth of *C. albicans*. Solid YPD-K (20 g/L peptone, 10 g/L yeast extract, 20 g/L glucose, 2.5 g/L K₂HPO₄, 20 g/L agar) and YP-K (20 g/L peptone, 10 g/L yeast extract, 2.5 g/L K₂HPO₄, 20 g/L agar) media were used for mating-projection induction assays. Peptone, yeast extract, and agar were purchased from BD Biosciences (BD Bacto, Cat. Nos., 211677, 212750, G8270, and 214010; BD Biosciences, Sparks, MD, USA). Glucose, phloxine B, and K₂HPO₄ were purchased from Sigma-Aldrich (Cat. Nos., G8270, P2759, and P9666; Sigma-Aldrich, St. Louis, MO, USA). The pH of YPD-K and YP-K media were about 7.3. Opaque cells were used for all mating and mating projection formation assays.

Sorbitol medium was made according to a previous study [48]. YPD-K, YP-K, agar-only (3%), agar + *C. albicans* debris, or agar + 3% mouse feces media were used for quantitative mating assays. To make the *C. albicans* debris medium, approximately 1×10^{10} cells of SC5314 were collected from an overnight YPD culture, washed with ddH₂O, frozen at -80°C, and ground with glass beads. Cell debris and 2% agar were mixed and resuspended in 100 mL

ddH₂O for autoclaving. To make the mouse feces medium, 2% agar and 3% mouse feces (w/v) were mixed and resuspended in ddH₂O. Before subjecting to autoclaving, 0.25% K₂HPO₄ was added to the agar-only (3%), agar + *C. albicans* debris, or agar + 3% mouse feces media for pH buffering. Synthetic complete medium (SCD) lacking corresponding nutrients (uridine, histidine [His], and/or arginine [Arg]) was used for selectable growth in quantitative mating assays.

To make H₂O₂-containing YPD-K medium, 200 μl of 5 mM H₂O₂ was spread onto YPD-K medium plates. Opaque cells of GH1350a were first grown on Lee's glucose medium at 25°C for three days. 1 × 10⁶ cells in 10 μL of ddH₂O were spotted onto different H₂O₂-containing YPD-K media and cultured at 25°C for three to five days.

Construction of plasmids

To inactivate the *SacII* site of *tetON*-promoter-containing plasmid pNIM1 [49], the plasmid was first digested with *SacII* and then filled in with the Klenow fragment of DNA polymerase I. The blunt ends were ligated to generate the *SacII*-free plasmid pNIMsx. To construct the plasmids pNIMsx-HSP90con and pNIMsx-HSF1con for conditional knockout of *HSP90* and *HSF1*, respectively, one fragment of partial ORF region of *HSP90* or *HSF1* (with *SallI* and *SacII* sites) and another fragment of the corresponding 5'-UTR region (with *SacII* and *BglIII* sites) were simultaneously subcloned into the *SallI* and *BglIII* sites and replaced the GFP cassette.

To construct the nourseothricin-resistant plasmid pACTS, a *caSAT1* fragment was amplified from pNIM1 [49] and subcloned into the *HindIII/KpnI* site of pACT1 [50]. A fragment containing the *MTLa2* ORF region was then subcloned into the *EcoRV/HindIII* site of pACTS, generating the overexpressing plasmid pACTS-MTLa2.

To create a Myc-tagged *Cwt1* plasmid, the *CdHIS1* cassette was amplified from plasmid pSN52 and inserted into plasmid pACT1 at the *ClaI* site, generating plasmid pACT1-HIS1. A fusion PCR product containing the *CWT1* ORF region and a C-terminal 13× Myc tag were prepared and subcloned into the *EcoRV/KpnI* site of pACT1-HIS1, yielding plasmid pACT1-CWT1-Myc-HIS1.

A *TAP-ARG4* cassette flanked by approximately 70-bp-5'– and 3'–homologous sequences of *CWT1* was amplified from strain CaLC2993 with primer pair LT1266 and LT1267 and was then transformed into the WT strain SN95 (CaLC239) to create TAP-tagged strain LTS1036 [51, 52]. The fragment containing the *CWT1* ORF region and a C-terminal TAP-ARG4 tag was amplified from strain LTS1036 with oligonucleotides LT1271/LT1272 and then subcloned into the *EcoRV/KpnI* site of pACT1 [50], generating plasmid pACT-CWT1-TAP-ARG4.

A *TAP-ARG4* cassette flanked by approximately 70-bp-5'– and 3'–homologous sequences of *CTA4* was amplified from strain CaLC2993 with primer pair LT1459 and LT1460 and was then transformed into the WT strain SN95 (CaLC239) to create TAP-tagged strain LTS1071 [52]. The fragment containing the *CTA4* ORF region and a C-terminal TAP-ARG4 tag were amplified from strain LTS1071 with oligonucleotides LT1271/LT1462 and then subcloned into the *EcoRV/KpnI* site of pACT1, generating plasmid pACT-CTA4-TAP-ARG4.

Construction of *C. albicans* strains

To construct the conditional knockout mutants of *HSP90* in strain GH1013, we first replaced the promoter of one allele with the *tetON* promoter using *SacII*-digested plasmid pNIMsx-HSP90con, generating mutant *tetON-HSP90/HSP90*. The other allele of *HSP90* was then replaced with the *ARG4* cassette amplified from pRS-ARG4ΔSpeI [53] with oligonucleotides HSP90-5DR/HSP90-3DR, generating the conditional mutant *tetON-HSP90/hsp90*. Since opaque cells of the *tetON-HSP90/hsp90* mutant were not stable, the master regulator *WOR1*

was overexpressed in this mutant using plasmid pACT1-WOR1 [50]. To construct the conditional knockout mutant of *HSF1*, we deleted the first allele in strain GH1013 using the *URA3* cassette amplified from pGEM-*URA3* [53] with oligonucleotides HSF1-5DR/HSF1-3DR, generating the mutant *hsf1::URA3/HSF1*. Then, we replaced the promoter region of the second allele of *HSF1* with the *tetON* promoter using *SacII*-digested plasmid pNIMsx-*HSF1con*, generating the mutant *tetON-HSF1/hsf1*. The *cartTA* cassette (reverse *tet* repressor) is under the control of the white-cell-specific *ADH1* promoter in the plasmid pNIM1 [49]. To increase the expression level of *cartTA* in opaque cells, the cassette was integrated into the opaque-specific *OP4* locus in the *tetON-HSF1/hsf1* and *tetON-HSP90/hsp90* mutants by transformation with fusion PCR products of *cartTA-ARG4*. pNIM1 and pRS-*ARG4*Δ*SpeI* were used as the primary template.

To delete both alleles of *CWT1*, the *HIS1* and *ARG4* markers flanked by *CWT1* gene 5'- and 3'-fragments were amplified with fusion PCR assays and sequentially transformed into strain GH1013 as described previously [53]. The plasmids pGEM-*HIS1* and pRS-*ARG4*Δ*SpeI* were used as the PCR templates. All oligonucleotides used are listed in S3 Table.

To determine Cwt1-binding targets, a TAP-tagged Cwt1-ecotopic strain was constructed. The plasmid pACT-CWT1-TAP-*ARG4* was linearized with *AscI* and transformed into strain SN95 [54] to create a TAP-tagged Cwt1-overexpressing strain (LTS1039). The function of TAP-tagged Cwt1 was verified by mating projection formation assays. To construct the *MTLa2*-overexpressing strain, plasmid pACTS-*MTLa2* was linearized with *AscI* and transformed into strain GH1350a.

To construct a TAP-tagged Cta4-ecotopic expression strain, the plasmid pACT-CTA4-TAP-*ARG4* was linearized with *AscI* and transformed into strain SN95 to create TAP-tagged CTA4-ecotopic expression strain (LTS1079). To construct a GFP-tagged Hsp90 strain, a *HSP90-GFP-SAT1* fusion fragment into the pACT1 plasmid [50], generating plasmid pACT1-HSP90-GFP-SAT1. The plasmids pACT1-HSP90-GFP-SAT1 and pACT1-CWT1-Myc-*HIS1* were linearized with *AscI* and subsequently transformed into strain SN95 [54], yielding strain LTS1062 with a GFP-tagged HSP90 and 13× Myc-tagged *CWT1* allele.

Construction of GFP-reporter strains

To construct the *MFa1p*-GFP, *MFαp*-GFP, *FIG1p*-GFP, and *FUS1p*-GFP reporter strains, GH1013 was transformed with PCR products of the *GFP-caSAT1* cassette amplified from plasmid pNIM1 with corresponding primers. The forward and reverse primers contain a 60-bp flanking sequence homologous to the promoter and 3'-UTR regions of *MFa1*, *MFα*, *FIG1*, or *FUS1*, respectively. Correct integration of the transformations was verified with PCR assays.

Quantitative mating assay

Same-sex mating assays were performed according to our previous publications with slight modifications [55]. Briefly, opaque cells of two “a” strains (1×10^7 for each) were mixed, spotted onto different media, and cultured at 25°C for three to seven days as indicated in the main text. Mating mixtures were then replated onto SCD-His, -Arg, -uridine, -His-Arg, or -Arg-uridine dropout media for prototrophic selection growth. Colonies grown out on the three types of plates were counted, and mating efficiency was calculated.

Flow cytometry analysis

C. albicans cells were incubated in liquid SCD medium with shaking at 30°C overnight, harvested, washed, and resuspended in 1× TE buffer (10 mM Tris, 1 mM EDTA [pH 8.0]). Cells were then fixed with 70% ethanol for two hours at room temperature and washed with 1× TE

buffer before treating with 1 mg/mL RNase A and 5 mg/ml proteinase K. Propidium iodide (PI, 25 µg/ml) staining assays were then performed. Stained cells were washed and resuspended in 1× TE buffer for DNA content analysis. A total of approximately 30,000 cells of each sample were used for flow cytometry assays, and the results were analyzed using software FlowJo 7.6.1.

Quantitative real-time PCR and RNA-Seq assays

Quantitative real-time PCR assays were performed according to our previous publications with modifications [56]. Cells were collected from cultures grown on solid plates as described in the main text. One µg of total RNA per sample was used to synthesize cDNA with RevertAid H Minus Reverse Transcriptase (Thermo Scientific, Waltham, MA, USA). Quantification of transcripts was performed in Bio-Rad CFX96 real-time PCR detection system using SYBR green. The signal from each experimental sample was normalized to expression of the *ACT1* gene.

For RNA-Seq assays, opaque cells of *C. albicans* were grown to stationary phase on Lee's glucose medium at 25°C for five days and then spotted onto YPD-K and YP-K medium at 25°C for 60 hours of incubation. Two biological repeats were performed for each condition. Cells were harvested, and total RNA was extracted. RNA-Seq analysis was performed by the company Berry Genomics (Beijing, China) as described previously [57]. Briefly, approximately 10 million (M) reads were sequenced in each library of the samples. The library products were then sequenced using an Illumina HiSeq 2500 V4 (Illumina, San Diego, CA, USA). Illumina software OLB_1.9.4 was used for base calling. The raw reads were filtered by removing the adapter and low-quality reads (the percentage of low-quality bases with a quality value ≤ 3 was $>50\%$ in a read). Clean reads were mapped to the genome of *C. albicans* SC5314 using TopHat (version 2.1.1) and Cufflinks (version 2.2.1) software [58]. Relative gene expression levels were calculated using the fragments per kb per million reads (FPKM) method. To be considered significantly differentially expressed, a gene must satisfy three criteria: (1) an FPKM value higher than or equal to 20 at least in one sample, (2) a fold change value higher than or equal to 1.5 (except for the Functional categories sheet of [S1 Data](#), in which a 2-fold change cutoff was used), and (3) an adjusted *p*-value (false discovery rate [FDR]) lower than 0.05.

Chromatin IP and co-IP assays

ChIP assays were performed as described previously [52, 59]. Briefly, untagged (CaLC239, SN95) and pACT1-Cwt1-TAP-tagged (LTS1039) *C. albicans* strains were spotted on YP-K medium and incubated at 25°C for one and three days. Cells were collected and fixed in 1× PBS containing 1% formaldehyde and incubated with gentle rocking for 20 min at room temperature. The crosslinking reaction was quenched by adding 2.5 M glycine to a final concentration of 125 mM, and cells were mixed for 5 min at room temperature. Cells were harvested, washed with 1× PBS, and homogenized in ice-cold lysis buffer using a bead beater. Sonication was performed with a Diagenode Bioruptor (Diagenode, Denville, NJ, USA) (12 min, high setting, 30 s on, 1 min off) to obtain chromatin fragments of an average size of 250–1,000 bp. The chromatin was immunoprecipitated with 50 µl packed IgG Sepharose 6 Fast Flow matrix (GE Healthcare, Chicago, IL, USA). The Sepharose matrix was washed, and immunoprecipitated chromatin DNA was eluted and de-crosslinked at 65°C overnight. Quantitative real-time PCR assays were performed to determine Cwt1 targets.

Cells grown on YP-K and YPD-K media were harvested and suspended in lysis buffer containing 50 mM Na-HEPES (pH 7.5), 450 mM NaOAc (pH 7.5), 1 mM EDTA, 1 mM EGTA, 5 mM MgOAc, 5% glycerol, 0.25% NP-40, 3 mM DTT, 1 mM PMSF, and EDTA-free protease

inhibitor mix (Cat. No., 11873580001; Roche Diagnostics, Mannheim, Germany). Cells were lysed using a beadbeating instrument by five rounds of beating (50 s beating plus 1 min cooling process on ice for each round). The supernatant of cell lysates was collected and incubated with Sepharose beads conjugated anti-GFP monoclonal antibody at 4°C for three hours. The beads were washed for four times with the lysis buffer and then boiled for 10 min in 1× sodium dodecyl sulfate (SDS) sample buffer. Immunoprecipitated proteins were separated through an SDS-10% polyacrylamide gel and used for western blotting analysis using anti-Myc monoclonal antibodies (Cat. No., OP10; MilliporeSigma, Billerica, MA, USA).

Intracellular ROS determination

Cells were cultured for one to five days on YP-K or YPD-K medium at 25°C. Cells were then harvested and washed in 1 × PBS and incubated with DCFDA (Beyotime, Shanghai, China) for 30 min at 37°C. After washing, fluorescence intensity reflecting the ROS level was measured at 488 nm using ELISA and was normalized according to the cell numbers.

Supporting information

S1 Fig. Development of polarized growth under different glucose concentrations. 1×10^7 cells of strain GH1350a were spotted on media containing different levels of glucose and cultured at 25°C for three or seven days. Percentages of projected cells are indicated in the corresponding images. The percentage of projected cells decreases with the increase of glucose level. (TIF)

S2 Fig. Expression of mating-related genes in GFP-reporter strains under glucose starvation conditions. 1×10^5 cells of each GFP-tagged strain (GH1013 background) were spotted on YP-K or YPD-K medium and cultured at 25°C for five days. Scale bar, 10 μm. DIC, differential interference contrast; GFP, green fluorescent protein; YPD-K, yeast extract-peptone-glucose- K_2HPO_4 ; YP-K, yeast extract-peptone- K_2HPO_4 . (TIF)

S3 Fig. Same-sex mating of *C. albicans* under conditions mimicking natural environments. (A) Diagram of experimental procedures. (B, C, and D) Mating efficiency on 3% agar without additional nutrients (B), on agar containing 3% mouse feces (C), and agar containing *C. albicans* debris (D). 1×10^7 cells of GH1013 and 1×10^7 cells of GH1350a were mixed and cultured on different medium plates at 25°C for three to seven days. Mating mixtures were replated onto SCD-Arg, SCD-His, and both dropout plates for selectable growth and mating efficiency calculation. For mating on agar without additional nutrients (B), a portion of cells underwent cell death and released nutrients for the survived cells. (E) Mating on sorbitol medium (opaque filamentation inducing medium). The numerical data are presented in **S3 Data**. Arg, arginine; His, histidine; SCD, synthetic complete medium. (TIF)

S4 Fig. Relative expression levels of *HSF1* and *HSP90* and FACS analysis of mating progeny. (A) Relative transcriptional expression levels of *HSF1* or *HSP90* in the control and *tetON-HSF1/hsf1* or *tetON-HSP90/hsp90* mutant on YP-K and YPD-K media with or without doxycycline (40 μg/mL). 1×10^5 cells were spotted on YP-K or YPD-K medium and cultured at 25°C for three days. Error bars, standard errors of technical duplicates * $p < 0.05$, two-tailed Student *t* test. Experiment was performed in biological replicate and representative image is shown. (B) FACS analysis of the DNA content of progeny strains. Parental strain GH1350a used as a diploid control. Mating progeny contain DNA content corresponding to 4C and 8C peaks confirming their tetraploid nature. This figure is related to the quantitative results

presented in supplementary [S1 Table](#). The numerical data are presented in [S3 Data](#). FACS, Fluorescence-activated cell sorting; Hsf1, Heat Shock transcription Factor 1; Hsp90, Heat shock protein 90; *tetON*, tetracycline-induced; *tetON-HSF1/hsf1*, *tetON*-promoter-controlled conditional expression strain of *HSF1*; YPD-K, yeast extract-peptone-glucose-K₂HPO₄; YP-K, yeast extract-peptone-K₂HPO₄.
(TIF)

S5 Fig. Identification of the *cwt1/cwt1* mutant by screening a transcription factor mutant library of *C. albicans*. (A) Formation mating projections in the *cwt1/cwt1* mutant on YPD-K and YP-K media. 1×10^5 cells of each strain were spotted on different media and cultured at 25°C for three or five days. Scale bar for colonies, 2 mm; scale bar for cells, 10 μm. (B) Relative expression levels of mating-related genes in the control (GH1350a) and *cwt1/cwt1* mutant on YPD-K and YP-K media. Error bars, standard errors. * $p < 0.05$, two-tailed Student *t* test. Two biological and two technical repeats were performed, respectively. The numerical data are presented in [S3 Data](#). Cwt1, Cell Wall Transcription factor 1; p, mating projection; YPD-K, yeast extract-peptone-glucose-K₂HPO₄; YP-K, yeast extract-peptone-K₂HPO₄.
(TIF)

S6 Fig. Identification of the *cta4/cta4* mutant by screening a transcription factor mutant library of *C. albicans*. (A) Colony and cellular morphologies of the control (WT, GH1350a) and *cta4/cta4* mutant on YP-K medium. 1×10^5 cells of each strain were spotted on different media and cultured at 25°C for five days. Scale bar for colonies, 2 mm; scale bar for cells, 10 μm. (B) Relative expression levels of *CWT1* and mating-related genes in the control (GH1350a) and *cta4/cta4* mutant on YPD-K and YP-K media. Cells of *C. albicans* used for qRT-PCR assays were cultured at 25°C for five days. Error bars, standard errors. * $p < 0.05$, two-tailed Student *t* test. Two biological and two technical repeats were performed, respectively. (C) Cta4 binds to the promoters of *CWT1*. ChIP assays were performed in TAP-tagged Cta4 strains. Cells of *C. albicans* used for ChIP assays were grown on YP-K or YPD-K medium at 25°C for 24 hours. Percentages of input genomic DNA are indicated. Dark arrows indicate detected promoter regions. d1, d2, and d3, three detected sites of *CWT1*. Error bars represent standard error of two technical replicates. * $p < 0.05$, two-tailed Student *t* test. Experiment was performed in biological replicate with a representative image shown. The numerical data are presented in [S3 Data](#). ChIP, chromatin immunoprecipitation; Cta4, *Candida* TransActivating protein 4; Cwt1, Cell Wall Transcription factor 1; p, mating projection; qRT-PCR, quantitative reverse transcription PCR; WT, wild type; YPD-K, yeast extract-peptone-glucose-K₂HPO₄; YP-K, yeast extract-peptone-K₂HPO₄.
(TIF)

S1 Table. Efficiency of same-sex mating in the *tetON-HSF1/hsf1*, *tetON-HSP90/hsp90* and *cwt1/cwt1* mutants. Cwt1, Cell Wall Transcription factor 1; Hsf1, Heat Shock transcription Factor 1; Hsp90, Heat shock protein 90; *tetON*, tetracycline-induced; *tetON-HSF1/hsf1*, *tetON*-promoter-controlled conditional expression strain of *HSF1*.
(DOC)

S2 Table. Strains used in this study.
(XLSX)

S3 Table. Primers used in this study.
(XLS)

S1 Data. RNA-Seq dataset. RNA-Seq, RNA sequencing
(XLSX)

S2 Data. HSP90 genetic interactors that differentially expressed in YP-K and YPD-K media. Hsp90, Heat shock protein 90; YPD-K, yeast extract-peptone-glucose-K₂HPO₄; YP-K, yeast extract-peptone-K₂HPO₄
(XLSX)

S3 Data. Excel files containing the underlying numerical data for Figs 1C, 3A, 3C, 3D, 5B, 6B, 7C, 7D, 8AC, S3B, S3C, S3D, S3E, S4A, S5B, S6B and S6C.
(XLSX)

Acknowledgments

The authors thank Drs. Suzanne Noble and Joachim Morschhäuser for the generous gifts of plasmids and strains.

Author Contributions

Conceptualization: Guobo Guan, Leah E. Cowen, Guanghua Huang.

Data curation: Guobo Guan, Li Tao, Jiao Gong, Jian Bing, Qiushi Zheng, Amanda O. Veri, Guanghua Huang.

Formal analysis: Guobo Guan, Li Tao, Huizhen Yue, Weihong Liang, Jiao Gong, Jian Bing, Qiushi Zheng, Amanda O. Veri, Nicole Robbins, Leah E. Cowen, Guanghua Huang.

Funding acquisition: Guanghua Huang.

Investigation: Guobo Guan, Li Tao, Huizhen Yue, Weihong Liang, Jiao Gong, Jian Bing, Amanda O. Veri, Shuru Fan, Guanghua Huang.

Methodology: Guobo Guan, Li Tao, Huizhen Yue, Weihong Liang, Jiao Gong, Jian Bing, Qiushi Zheng, Amanda O. Veri, Shuru Fan.

Project administration: Guanghua Huang.

Resources: Weihong Liang, Shuru Fan.

Supervision: Guanghua Huang.

Validation: Guobo Guan, Li Tao, Weihong Liang, Jiao Gong, Jian Bing, Qiushi Zheng, Shuru Fan, Nicole Robbins, Leah E. Cowen, Guanghua Huang.

Writing – original draft: Guobo Guan, Huizhen Yue, Jiao Gong, Jian Bing, Guanghua Huang.

Writing – review & editing: Guobo Guan, Amanda O. Veri, Nicole Robbins, Leah E. Cowen, Guanghua Huang.

References

1. Lee SC, Ni M, Li W, Shertz C, Heitman J. The evolution of sex: a perspective from the fungal kingdom. *Microbiol Mol Biol Rev.* 2010; 74(2):298–340. <https://doi.org/10.1128/MMBR.00005-10> PMID: 20508251; PubMed Central PMCID: PMC2884414.
2. Gow NA. Fungal biology: Multiple mating strategies. *Nature.* 2013; 494(7435):45–6. <https://doi.org/10.1038/nature11945> PMID: 23364693.
3. Pfaller MA, Diekema DJ. Epidemiology of invasive candidiasis: a persistent public health problem. *Clinical microbiology reviews.* 2007; 20(1):133–63. <https://doi.org/10.1128/CMR.00029-06> PMID: 17223626; PubMed Central PMCID: PMC1797637.

4. Hull CM, Raisner RM, Johnson AD. Evidence for mating of the "asexual" yeast *Candida albicans* in a mammalian host. *Science*. 2000; 289(5477):307–10. PMID: [10894780](#).
5. Magee BB, Magee PT. Induction of mating in *Candida albicans* by construction of MTL α and MTL α strains. *Science*. 2000; 289(5477):310–3. Epub 2000/07/15. 8662 [pii]. PMID: [10894781](#).
6. Bennett RJ, Johnson AD. Completion of a parasexual cycle in *Candida albicans* by induced chromosome loss in tetraploid strains. *The EMBO journal*. 2003; 22(10):2505–15. <https://doi.org/10.1093/emboj/cdg235> PMID: [12743044](#); PubMed Central PMCID: PMCPMC155993.
7. Forche A, Alby K, Schaefer D, Johnson AD, Berman J, Bennett RJ. The parasexual cycle in *Candida albicans* provides an alternative pathway to meiosis for the formation of recombinant strains. *PLoS Biol*. 2008; 6(5):e110. <https://doi.org/10.1371/journal.pbio.0060110> PMID: [18462019](#); PubMed Central PMCID: PMC2365976.
8. Miller MG, Johnson AD. White-opaque switching in *Candida albicans* is controlled by mating-type locus homeodomain proteins and allows efficient mating. *Cell*. 2002; 110(3):293–302. Epub 2002/08/15. S0092867402008371 [pii]. PMID: [12176317](#).
9. Johnson A. The biology of mating in *Candida albicans*. *Nat Rev Microbiol*. 2003; 1(2):106–16. <https://doi.org/10.1038/nrmicro752> PMID: [15035040](#).
10. Soll DR. Why does *Candida albicans* switch? *FEMS Yeast Res*. 2009; 9(7):973–89. Epub 2009/09/12. <https://doi.org/10.1111/j.1567-1364.2009.00562.x> PMID: [19744246](#).
11. Huang G. Regulation of phenotypic transitions in the fungal pathogen *Candida albicans*. *Virulence*. 2012; 3(3):251–61. <https://doi.org/10.4161/viru.20010> PMID: [22546903](#); PubMed Central PMCID: PMCPMC3442837.
12. Noble SM, Gianetti BA, Witchley JN. *Candida albicans* cell-type switching and functional plasticity in the mammalian host. *Nat Rev Microbiol*. 2017; 15(2):96–108. <https://doi.org/10.1038/nrmicro.2016.157> PMID: [27867199](#).
13. Graser Y, Volovsek M, Arrington J, Schonian G, Presber W, Mitchell TG, et al. Molecular markers reveal that population structure of the human pathogen *Candida albicans* exhibits both clonality and recombination. *Proc Natl Acad Sci U S A*. 1996; 93(22):12473–7. PMID: [8901606](#); PubMed Central PMCID: PMCPMC38016.
14. Odds FC, Bognoux ME, Shaw DJ, Bain JM, Davidson AD, Diogo D, et al. Molecular phylogenetics of *Candida albicans*. *Eukaryot Cell*. 2007; 6(6):1041–52. <https://doi.org/10.1128/EC.00041-07> PMID: [17416899](#); PubMed Central PMCID: PMCPMC1951527.
15. Butler G, Kenny C, Fagan A, Kurischko C, Gaillardin C, Wolfe KH. Evolution of the MAT locus and its Ho endonuclease in yeast species. *Proc Natl Acad Sci U S A*. 2004; 101(6):1632–7. <https://doi.org/10.1073/pnas.0304170101> PMID: [14745027](#); PubMed Central PMCID: PMCPMC341799.
16. Alby K, Schaefer D, Bennett RJ. Homothallic and heterothallic mating in the opportunistic pathogen *Candida albicans*. *Nature*. 2009; 460(7257):890–3. <https://doi.org/10.1038/nature08252> PMID: [19675652](#); PubMed Central PMCID: PMC2866515.
17. Forche A, Abbey D, Pisithkul T, Weinzierl MA, Ringstrom T, Bruck D, et al. Stress alters rates and types of loss of heterozygosity in *Candida albicans*. *mBio*. 2011; 2(4): e00129–11. <https://doi.org/10.1128/mBio.00129-11> PMID: [21791579](#); PubMed Central PMCID: PMCPMC3143845.
18. Alby K, Bennett RJ. Stress-induced phenotypic switching in *Candida albicans*. *Mol Biol Cell*. 2009; 20(14):3178–91. <https://doi.org/10.1091/mbc.E09-01-0040> PMID: [19458191](#); PubMed Central PMCID: PMC2710840.
19. Brown AJ, Brown GD, Netea MG, Gow NA. Metabolism impacts upon *Candida* immunogenicity and pathogenicity at multiple levels. *Trends Microbiol*. 2014; 22(11):614–22. <https://doi.org/10.1016/j.tim.2014.07.001> PMID: [25088819](#); PubMed Central PMCID: PMCPMC4222764.
20. Huang G, Yi S, Sahni N, Daniels KJ, Srikantha T, Soll DR. N-acetylglucosamine induces white to opaque switching, a mating prerequisite in *Candida albicans*. *PLoS Pathog*. 2010; 6(3):e1000806. Epub 2010/03/20. <https://doi.org/10.1371/journal.ppat.1000806> PMID: [20300604](#); PubMed Central PMCID: PMC2837409.
21. Lockhart SR, Daniels KJ, Zhao R, Wessels D, Soll DR. Cell biology of mating in *Candida albicans*. *Eukaryot Cell*. 2003; 2(1):49–61. <https://doi.org/10.1128/EC.2.1.49-61.2003> PMID: [12582122](#); PubMed Central PMCID: PMCPMC141171.
22. Baker BM, Haynes CM. Mitochondrial protein quality control during biogenesis and aging. *Trends in biochemical sciences*. 2011; 36(5):254–61. <https://doi.org/10.1016/j.tibs.2011.01.004> PMID: [21353780](#).
23. Diezmann S, Michaut M, Shapiro RS, Bader GD, Cowen LE. Mapping the Hsp90 genetic interaction network in *Candida albicans* reveals environmental contingency and rewired circuitry. *PLoS Genet*. 2012; 8(3):e1002562. <https://doi.org/10.1371/journal.pgen.1002562> PMID: [22438817](#); PubMed Central PMCID: PMC3305360.

24. O'Meara TR, Veri AO, Polvi EJ, Li X, Valaei SF, Diezmann S, et al. Mapping the Hsp90 Genetic Network Reveals Ergosterol Biosynthesis and Phosphatidylinositol-4-Kinase Signaling as Core Circuitry Governing Cellular Stress. *PLoS Genet.* 2016; 12(6):e1006142. <https://doi.org/10.1371/journal.pgen.1006142> PMID: 27341673; PubMed Central PMCID: PMC4920384.
25. Verghese J, Abrams J, Wang Y, Morano KA. Biology of the heat shock response and protein chaperones: budding yeast (*Saccharomyces cerevisiae*) as a model system. *Microbiol Mol Biol Rev.* 2012; 76(2):115–58. <https://doi.org/10.1128/MMBR.05018-11> PMID: 22688810; PubMed Central PMCID: PMC3372250.
26. O'Meara TR, Cowen LE. Hsp90-dependent regulatory circuitry controlling temperature-dependent fungal development and virulence. *Cellular microbiology.* 2014; 16(4):473–81. <https://doi.org/10.1111/cmi.12266> PMID: 24438186.
27. Liu XD, Thiele DJ. Oxidative stress induced heat shock factor phosphorylation and HSF-dependent activation of yeast metallothionein gene transcription. *Genes Dev.* 1996; 10(5):592–603. PMID: 8598289.
28. Hahn JS, Thiele DJ. Activation of the *Saccharomyces cerevisiae* heat shock transcription factor under glucose starvation conditions by Snf1 protein kinase. *J Biol Chem.* 2004; 279(7):5169–76. <https://doi.org/10.1074/jbc.M311005200> PMID: 14612437.
29. Du H, Guan G, Xie J, Cottier F, Sun Y, Jia W, et al. The transcription factor Flo8 mediates CO₂ sensing in the human fungal pathogen *Candida albicans*. *Mol Biol Cell.* 2012; 23(14):2692–701. Epub 2012/05/25. <https://doi.org/10.1091/mbc.E12-02-0094> PMID: 22621896; PubMed Central PMCID: PMC3395658.
30. Sellam A, Tebbji F, Whiteway M, Nantel A. A novel role for the transcription factor Cwt1p as a negative regulator of nitrosative stress in *Candida albicans*. *PLoS ONE.* 2012; 7(8):e43956. <https://doi.org/10.1371/journal.pone.0043956> PMID: 22952822; PubMed Central PMCID: PMC3430608.
31. Antonsson C, Whitelaw ML, McGuire J, Gustafsson JA, Poellinger L. Distinct roles of the molecular chaperone hsp90 in modulating dioxin receptor function via the basic helix-loop-helix and PAS domains. *Mol Cell Biol.* 1995; 15(2):756–65. PMID: 7823943; PubMed Central PMCID: PMC3395658.
32. Liu YV, Baek JH, Zhang H, Diez R, Cole RN, Semenza GL. RACK1 competes with HSP90 for binding to HIF-1 α and is required for O₂-independent and HSP90 inhibitor-induced degradation of HIF-1 α . *Molecular cell.* 2007; 25(2):207–17. <https://doi.org/10.1016/j.molcel.2007.01.001> PMID: 17244529; PubMed Central PMCID: PMC3395658.
33. Tsong AE, Miller MG, Raisner RM, Johnson AD. Evolution of a combinatorial transcriptional circuit: a case study in yeasts. *Cell.* 2003; 115(4):389–99. PMID: 14622594.
34. Moreno I, Castillo L, Sentandreu R, Valentin E. Global transcriptional profiling of *Candida albicans* cwt1 null mutant. *Yeast.* 2007; 24(4):357–70. <https://doi.org/10.1002/yea.1444> PMID: 17238235.
35. Feretzaki M, Heitman J. Unisexual reproduction drives evolution of eukaryotic microbial pathogens. *PLoS Pathog.* 2013; 9(10):e1003674. <https://doi.org/10.1371/journal.ppat.1003674> PMID: 24204257; PubMed Central PMCID: PMC3814335.
36. Nielsen K, De Obaldia AL, Heitman J. *Cryptococcus neoformans* mates on pigeon guano: implications for the realized ecological niche and globalization. *Eukaryot Cell.* 2007; 6(6):949–59. <https://doi.org/10.1128/EC.00097-07> PMID: 17449657; PubMed Central PMCID: PMC3395658.
37. Fabrizio P, Battistella L, Vardavas R, Gattazzo C, Liou LL, Diaspro A, et al. Superoxide is a mediator of an altruistic aging program in *Saccharomyces cerevisiae*. *The Journal of cell biology.* 2004; 166(7):1055–67. <https://doi.org/10.1083/jcb.200404002> PMID: 15452146; PubMed Central PMCID: PMC3395658.
38. Berman J, Hadany L. Does stress induce (para)sex? Implications for *Candida albicans* evolution. *Trends in genetics: TIG.* 2012; 28(5):197–203. <https://doi.org/10.1016/j.tig.2012.01.004> PMID: 22364928; PubMed Central PMCID: PMC3395658.
39. Bennett RJ, Johnson AD. Mating in *Candida albicans* and the search for a sexual cycle. *Annu Rev Microbiol.* 2005; 59:233–55. <https://doi.org/10.1146/annurev.micro.59.030804.121310> PMID: 15910278.
40. Bennett RJ, Johnson AD. The role of nutrient regulation and the Gpa2 protein in the mating pheromone response of *C. albicans*. *Mol Microbiol.* 2006; 62(1):100–19. <https://doi.org/10.1111/j.1365-2958.2006.05367.x> PMID: 16987174.
41. Hull CM, Heitman J. Genetics of *Cryptococcus neoformans*. *Annual review of genetics.* 2002; 36:557–615. <https://doi.org/10.1146/annurev.genet.36.052402.152652> PMID: 12429703.
42. Bernstein C, Johns V. Sexual reproduction as a response to H₂O₂ damage in *Schizosaccharomyces pombe*. *J Bacteriol.* 1989; 171(4):1893–7. PMID: 2703462; PubMed Central PMCID: PMC3395658.
43. Akerfelt M, Morimoto RI, Sistonen L. Heat shock factors: integrators of cell stress, development and life-span. *Nat Rev Mol Cell Biol.* 2010; 11(8):545–55. <https://doi.org/10.1038/nrm2938> PMID: 20628411; PubMed Central PMCID: PMC3395658.

44. Sun Y, Gadoury C, Hirakawa MP, Bennett RJ, Harcus D, Marciel A, et al. Deletion of a Yci1 Domain Protein of *Candida albicans* Allows Homothallic Mating in MTL Heterozygous Cells. *mBio*. 2016; 7(2): e00465–16. <https://doi.org/10.1128/mBio.00465-16> PMID: 27118591; PubMed Central PMCID: PMC4850264.
45. Ni M, Feretzaki M, Li W, Floyd-Averette A, Mieczkowski P, Dietrich FS, et al. Unisexual and heterosexual meiotic reproduction generate aneuploidy and phenotypic diversity de novo in the yeast *Cryptococcus neoformans*. *PLoS Biol*. 2013; 11(9):e1001653. <https://doi.org/10.1371/journal.pbio.1001653> PMID: 24058295; PubMed Central PMCID: PMC3769227.
46. Hirakawa MP, Chyou DE, Huang D, Slan AR, Bennett RJ. Parasex Generates Phenotypic Diversity de Novo and Impacts Drug Resistance and Virulence in *Candida albicans*. *Genetics*. 2017; 207(3):1195–211. <https://doi.org/10.1534/genetics.117.300295> PMID: 28912344; PubMed Central PMCID: PMC485676243.
47. Xie J, Tao L, Nobile CJ, Tong Y, Guan G, Sun Y, et al. White-opaque switching in natural MTL α /alpha isolates of *Candida albicans*: evolutionary implications for roles in host adaptation, pathogenesis, and sex. *PLoS Biol*. 2013; 11(3):e1001525. <https://doi.org/10.1371/journal.pbio.1001525> PMID: 23555196; PubMed Central PMCID: PMC3608550.
48. Si H, Hernday AD, Hirakawa MP, Johnson AD, Bennett RJ. *Candida albicans* White and Opaque Cells Undergo Distinct Programs of Filamentous Growth. *PLoS Pathog*. 2013; 9(3):e1003210. Epub 2013/03/19. <https://doi.org/10.1371/journal.ppat.1003210> PMID: 23505370; PubMed Central PMCID: PMC3591317.
49. Park YN, Morschhauser J. Tetracycline-inducible gene expression and gene deletion in *Candida albicans*. *Eukaryot Cell*. 2005; 4(8):1328–42. Epub 2005/08/10. 4/8/1328 [pii] <https://doi.org/10.1128/EC.4.8.1328-1342.2005> PMID: 16087738; PubMed Central PMCID: PMC1214539.
50. Huang G, Wang H, Chou S, Nie X, Chen J, Liu H. Bistable expression of WOR1, a master regulator of white-opaque switching in *Candida albicans*. *Proc Natl Acad Sci U S A*. 2006; 103(34):12813–8. Epub 2006/08/15. 0605270103 [pii] <https://doi.org/10.1073/pnas.0605270103> PMID: 16905649; PubMed Central PMCID: PMC1540355.
51. Leach MD, Budge S, Walker L, Munro C, Cowen LE, Brown AJ. Hsp90 orchestrates transcriptional regulation by Hsf1 and cell wall remodelling by MAPK signalling during thermal adaptation in a pathogenic yeast. *PLoS Pathog*. 2012; 8(12):e1003069. <https://doi.org/10.1371/journal.ppat.1003069> PMID: 23300438; PubMed Central PMCID: PMC3531498.
52. Leach MD, Farrer RA, Tan K, Miao Z, Walker LA, Cuomo CA, et al. Hsf1 and Hsp90 orchestrate temperature-dependent global transcriptional remodelling and chromatin architecture in *Candida albicans*. *Nature communications*. 2016; 7:11704. <https://doi.org/10.1038/ncomms11704> PMID: 27226156; PubMed Central PMCID: PMC4894976.
53. Wilson RB, Davis D, Mitchell AP. Rapid hypothesis testing with *Candida albicans* through gene disruption with short homology regions. *J Bacteriol*. 1999; 181(6):1868–74. Epub 1999/03/12. PMID: 10074081; PubMed Central PMCID: PMC93587.
54. Noble SM, Johnson AD. Strains and strategies for large-scale gene deletion studies of the diploid human fungal pathogen *Candida albicans*. *Eukaryot Cell*. 2005; 4(2):298–309. Epub 2005/02/11. <https://doi.org/10.1128/EC.4.2.298-309.2005> PMID: 15701792; PubMed Central PMCID: PMC549318.
55. Tao L, Cao C, Liang W, Guan G, Zhang Q, Nobile CJ, et al. White cells facilitate opposite- and same-sex mating of opaque cells in *Candida albicans*. *PLoS Genet*. 2014; 10(10):e1004737. <https://doi.org/10.1371/journal.pgen.1004737> PMID: 25329547; PubMed Central PMCID: PMC4199524.
56. Cao C, Wu M, Bing J, Tao L, Ding X, Liu X, et al. Global regulatory roles of the cAMP/PKA pathway revealed by phenotypic, transcriptomic and phosphoproteomic analyses in a null mutant of the PKA catalytic subunit in *Candida albicans*. *Mol Microbiol*. 2017; 105(1):46–64. <https://doi.org/10.1111/mmi.13681> PMID: 28370450.
57. Tao L, Zhang Y, Fan S, Nobile CJ, Guan G, Huang G. Integration of the tricarboxylic acid (TCA) cycle with cAMP signaling and Sfl2 pathways in the regulation of CO₂ sensing and hyphal development in *Candida albicans*. *PLoS Genet*. 2017; 13(8):e1006949. <https://doi.org/10.1371/journal.pgen.1006949> PMID: 28787458; PubMed Central PMCID: PMC5567665.
58. Trapnell C, Roberts A, Goff L, Pertea G, Kim D, Kelley DR, et al. Differential gene and transcript expression analysis of RNA-seq experiments with TopHat and Cufflinks. *Nat Protoc*. 2012; 7(3):562–78. <https://doi.org/10.1038/nprot.2012.016> PMID: 22383036; PubMed Central PMCID: PMC43334321.
59. Nobile CJ, Fox EP, Nett JE, Sorrells TR, Mitrovich QM, Hernday AD, et al. A recently evolved transcriptional network controls biofilm development in *Candida albicans*. *Cell*. 2012; 148(1–2):126–38. Epub 2012/01/24. <https://doi.org/10.1016/j.cell.2011.10.048> PMID: 22265407; PubMed Central PMCID: PMC3266547.